Investigation of the Dosimetric Impact of Patient Immobilization Device and Treatment Couch Structures in Prone Breast Radiation Therapy

By

Amy Jessica Lau

05/22/2020

A dissertation submitted to the Faculty of the Graduate School of

the University at Buffalo, The State University of New York

in partial fulfillment of the requirements for the degree of

Doctor of Philosophy

Medical Physics Program

Jacobs School of Medicine and Biomedical Sciences

Acknowledgements

I would like to thank my advisor Dr. Iris Wang, for being there for me as my mentor. I really appreciate all the guidance and support that she has given me over the years. I would also like to thank my committee members Dr. Matthew Podgorsak, Dr. Lalith Kumaraswamy, Dr. Daniel Bednarek and Dr. Rutao Yao for their time and valuable input. I would like to thank the rest of the medical physics faculty, Dr. Stephen Rudin, Dr. Harish Malhotra, Dr. Daryl Nazareth, Dr. Anh Le and Professor Steve DeBoer for all their mentorship and teachings over the years. I want to also thank various Roswell Park staff members for their help and for being very open to sharing their clinical knowledge and experiences with me, in particular Rachel Hackett, Jeremy Garvin and Dr. Kilian Salerno (NIH). I would also like to thank Stephen Bhagroo and J Mathews for teaching me Monte Carlo. I want to thank all my friends in the program and past graduates for all the great times and support through the years. Lastly, I want to thank my parents and one of my best friends Amy Leung for their continuous support and encouragement.

Abstract

Purpose: In prone breast radiation, as the medial tangential beam usually passes through the immobilization board and couch, it is necessary to quantify the attenuation effect and the potential skin dose enhancement from these external structures when not included during the treatment planning process.

Methods: The prone breast board studied consists of an insert on which the contralateral breast rests and a board base indexed to the couch. Two different Varian couch systems were also studied. The three effects being quantified were attenuation, scatter and bolus effect. Transmission factors (TF) of the board were measured using a Farmer chamber at 4 cm depth. Couch TFs were measured using a thimble chamber centered in a cylindrical phantom. TFs were then computed in the treatment planning system (TPS) for comparison. Selected clinical plans were recomputed in the TPS incorporating external structures for target coverage evaluation. Skin dose effects were measured using a Markus parallel plate chamber with a 1 mm buildup cap. A custom support model was created in the TPS for clinical implementation. The correction for the attenuation effect incorporating the custom support and couch structures in the treatment plans was also demonstrated. Monte Carlo (MC) simulations were carried out on phantom studies to further investigate the scatter and bolus effects from the breast board. Finally, the work flow of incorporating external structures in MC simulation for clinical prone breast cases were presented where an example of a patient case utilizing this workflow was carried out for a TPS-MC comparison.

Results: Measured board insert / base TFs ranged 0.976-0.983 / 0.979-0.985 for 6MV and ranged 0.990-0.999 / 0.989-0.998 for 23MV x-rays, respectively, where TPS values agreed within 0.6%. Varian Exact Couch and Exact IGRT Couch TFs ranged 0.836-1 and 0.956-0.996, respectively, for 6 MV. The clinical treatment volume and whole breast receiving 95% of the prescription dose (CTV-V95 and WB-V95) of selected patients demonstrated reduced coverage due to attenuation of external structures. Close

proximity to the base increased skin dose by up to 25-30%. Contacting the insert increased skin dose by 65-93% for 6MV and 117-157% for 23MV, respectively. For the custom support model of the breast board, assigned Hounsfield units (HUs) providing the best agreement was 200 and -100/-900 for the insert and board base respectively. Measured and MC values were compared for scatter effect with varying assigned densities (i.e. 0.25 g/cm^3, 0.3 g/cm^3, "sandwich structure") where the "sandwich structure" showed the best agreement. A dose enhancement was also seen in the MC simulation of the bolus effect from the insert. The MC dose calculation of an example clinical case showed a hot spot in an area near the board insert.

Conclusion: Results have shown reduced coverage by attenuating external structures. Proper modeling of immobilization devices and couch structures in the TPS should be implemented for accurate dose calculation. Modelling a custom support structure in the TPS to match the measured attenuation results within a minimal margin of error is feasible. Increased surface doses were observed caused by direct contact to the insert or close proximity to the base. Further MC investigation with a sample of prone breast patients can potentially provide additional skin dose information for clinical decision.

Table of Contents

List of Tables

List of Figures

Chapter 1: Introduction

1.1 Breast Cancer and Staging

In the breast, carcinomas originate from the epithelial cells that line the ducts and acini (1). When multiplying malignant cells are confined within the basement membrane surrounding these ducts, acini or surface epithelium of the nipple, the tumor is also known as in situ carcinoma (1). When the basement membrane has been breached and these cells spread into the breast tissue, it is called invasive carcinoma (1). The two main histological types of in situ carcinoma are ductal and lobular carcinoma in situ (1).

A cancer is staged in accordance to the spread of the cancer when it is diagnosed. Usually breast cancer is staged using the American Joint Committee on Cancer (AJCC) TNM system. As of 2018, the latest AJCC system includes a clinical and pathologic staging systems (2). The pathologic or surgical stage is determined by tissues excised in surgery. The clinical stage is used when surgery cannot be performed immediately and the stage is determined from information obtained from tests and procedures. Pathalogic staging tends to be more accurate. The TNM system consists of assessing a tumor by its size (T), whether there is a regional lymph node involvement (N) and if there is any distant metastases (M) (2). Other information used in staging include estrogen receptor status, progesterone receptor status, Her2 status and grade of cancer (2). With all the previous information, an overall stage will be assigned. Following the TNM categorization, there are stages 0, I, II, III and IV with sub stages A, B and C. Stage 0 refers to an in situ stage, which includes ductal carcinoma in situ (DCIS), lobule carcinoma in situ (LCIS) and Paget disease of the nipple (2). Stage I refers to the local stage, II refers to either a local or regional stage that depends on lymph node involvement, III refers to the regional stage and IV refers to the distant stage (2). Local describes when the cancer is confined to the organ where it originated, regional describes when the cancer has spread to nearby tissues outside of the organ of origin or lymph nodes

are involved and distant describes when the cancer has spread to other parts of the body (2). Common areas for breast cancer metastasis are bones, liver, brain or lungs.

1.2 Breast Cancer Treatments

According to the Surveillance, Epidemiology, and End Results (SEER) program, the 5-year relative survival is 98.9%, 85.7% and 28.1% for localized, regional and distant stages respectively (3). Today there exist many treatment options for breast cancer depending on the type and stage. This includes local and systemic treatments such as surgery, radiation therapy, chemotherapy, hormone therapy and targeted therapy (1). In the past, the main treatment of breast cancer was a radical mastectomy regardless of tumour size or patient age which was introduced by Halsted in 1894 (4). Around 1930s, the idea of more conservative breast treatments appeared. Later on, conservative therapy was an established alternative to a mastectomy for treating early staged carcinomas in the breast (5). Breast conserving surgeries consist of two categories which are lumpectomy and partial mastectomy. A lumpectomy refers to the removal of the cancer with some tissue around it and a partial mastectomy includes the removal of the lining over the chest muscle in addition to the cancer and surrounding breast tissue (6). Several randomized studies have been performed showing that there were no significant differences in the outcome between conservative surgery with radiation and mastectomy alone (5,7). The National Surgical Adjuvant Breast and Bowel Project (NSABP) has also conducted randomized clinical trials in this area. The NSABP B-04 trial, after 25 years of follow up showed no significant differences in the survival of those who had a radical mastectomy and those treated with less extensive surgeries (8). The NSABP B-06 trial compared the treatment of women who had tumors of 4 cm or less with a lumpectomy alone, a lumpectomy with radiation and with total mastectomy (8). After 20 years of follow up, there are no significant differences in overall survival, disease free survival or distant disease free survival between

the three groups (8). It was also noted that between the groups who had a lumpectomy alone and those who had a lumpectomy with radiation, the likelihood of recurrence in the ipsilateral breast was reduced in those who had radiation (8).

1.3 Breast Radiation Therapy – Supine vs Prone Positioning

Traditionally, radiation therapy is delivered with opposed tangential photon beams (tangents) in the supine position. Radiation of 40-50 Gy is typically delivered to the whole breast after surgery and is then followed by a boost dose of 10-16 Gy to the surgery site or lumpectomy cavity with a clinical margin. In the past, pendulous breasts have been a contraindication for breast conservation therapy (BCT) due to a large medial lateral separation (i.e. tissue thickness) from the transverse displacement of breast tissue in the supine position. The large breast separation results in a non-uniform dose distribution and with this patient positioning a larger volume of normal tissue will be incorporated in the treatment fields (10). The pendulous breast group experienced more acute and late skin toxicities especially at the infra-mammary fold along with other late effects such as chronic fibrosis, retraction, telangiectasia and poorer cosmetic outcomes (11,12). Additionally, meta-analysis from the Early Breast Cancer Trialists' Collaborative Group has shown that women who have received treatment with supine tangents have excess late cardiac morbidity and mortality and lung cancer mortality (12). There have been several approaches for treatment of pendulous breasts which include combining beam energies, changing the treatment position and immobilization devices (11).

The prone breast radiation technique is an alternate method that was introduced to minimize the effects experienced by this group. In the prone position, the patient lies face down on a platform which has an aperture for the breast to fall away from the chest wall. Advantages of this position include minimizing skin folds, reducing normal tissues that are in the treatment field, improving dose

homogeneity and reducing motion from breathing. Figure 1-1 shows a comparison of the supine and prone position (34). Figure 1-1A shows the larger amount of normal tissue incoporated into the field.

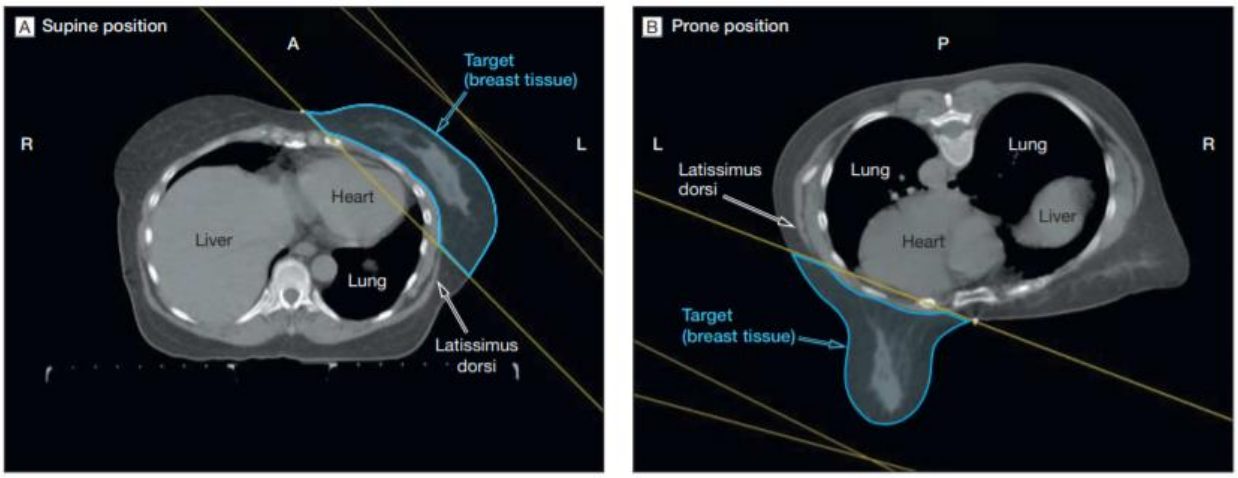

Figure 1-1: Comparison of a patient who benefitted from the prone position rather than supine. Adapted from Formenti SC, *et al*. Prone vs Supine Positioning for Breast Cancer Radiotherapy. *JAMA*. 2012;308(9):861–863.

1.4 Prone Breast Radiation – MSKCC Experience

In 1994, it was proposed by investigators from Memorial Sloan-Kettering Cancer Center (MSKCC) that prone breast was a possible alternative to the supine position to dealing with the limitations that came with treating women with large breast separations (10). The technique was a combination of the advantages of the decubitus treatment position and the reproducibility of the supine position (10). A commercially available platform that was based on the MSKCC experience was the Victoreen® Model 37-018 (11). The platform had an adjustable aperture that slid laterally and a wedge was placed on the contralateral side so the patient would rotate toward the ipsilateral breast. The ipsilateral arm was placed at the side or above the head. In the 1994 report, isodose distributions were shown for both the prone and supine position with beam wedges in the transverse plane and distributions in the prone position showed a more homogeneous distribution (10). In later reports, for patients treated from 1992 to 2004 it was shown that the prone technique was feasible and tolerable (11). The same group also

investigated the use of simplified IMRT prone breast technique with results that showed improved dose homogeneity. They also used the Canadian fractionation schedule (i.e. hypofractionation) which showed comparable results as conventional fractionation (11).

1.5 Prone Breast Radiation – USC Experience

Huppert *et al.* (11) described the research on accelerated partial breast radiation in the prone position in the early 1990's at the University of Southern California. The technique studied involved non-coplanar beams and was radiosurgery-like. The platform that was used was a wooden platform with removable inserts each with several concentric ring components for different sizes of the breast. The contralateral insert covered the opening while the ipsilateral breast would be centered in the other with the suitable rings. The arms would be placed at the side. Part of the board would extend from the treatment couch to allow couch rotation. The material of the board did not contain any metal to reduce CT artifacts and the thickness of the board was chosen so that it was sturdy when under a patient. The board was designed for partial breast treatments since there was tissue above the level of the opening and the beam would intersect with the arms and part of the wooden side bar. The described platform was used in a pilot study with ten patients, each of whom was treated with five fractions. Nine were treated with the proposed technique with multiple fixed fields using couch rotations. All patients received the five fractions over 10 days with the prescription dose ranging from 25-30 Gy. Three of them were assigned 5 Gy per fraction randomly, four were assigned 5.5 Gy and two were assigned 6.0 Gy. After a 36-53 month follow up, all patients were alive, disease free and with good cosmesis (11).

1.6 Prone Breast Radiation – NYU Experience

Huppert et al. (11) went further to discuss that research at New York University was directed towards the design of a device with prone whole breast radiation therapy. It was required that the method of immobilization had to be present during CT simulation and had to be exactly replicated in treatment. There were three designs for a new breast board. Version 1 was a board sharing similarities to the USC design. It had no metal frame and was extended over the treatment couch so that couch rotation would be possible. The arms of the patient would be placed above the head. When small tangential fields were used and an acceptable dose distribution was achievable, couch rotations were unnecessary. Version 2 allowed a more comfortable position for the patient. The board made of solid wood fully rested on the couch and included leg support which also permitted a thinner board to be used. In addition, a cushion could be placed on top for patient comfort. However, couch rotations were limited to less than 10 degrees. Version 3 incorporated a two inch thick layer of memory foam which rested on top of a 5 in Styrofoam™ which was wrapped in a vinyl cover. Additional layers of Styrofoam™ could be used for patients with larger breasts and placed under the mattress. The memory foam allowed higher reproducibility for patients over multiple sessions. Although version 3 of the breast board was light, affordable and easily transported, it had certain disadvantages such as no holding bars for the arms and no indexing capability to the couch. Therefore, it required experienced therapists and accurate lasers to avoid variations in setup. Later on, NYU provided their feedback of prone positioning designs to some commercial prone breast immobilization devices such as ClearVue™ (Orbital Therapy Inc.) and Access360™ (Varian Medical Systems Inc.). NYU also had clinical trials that tested hypofractionation schedules. They also carried out the first trial testing partial breast accelerated fractionation. All patients were treated with three-dimensional conformal radiotherapy after breast conservation surgery. In 2002, NYU began a phase I-II trial of prone accelerated intensity modulated radiation therapy to the whole

breast plus a boost to the tumor bed. Results of the trial demonstrated that the technique was feasible for all patients independent of the volume of the breast and also allowed for lung and heart sparing (11).

1.7 Hypofractionated Breast Radiation Therapy

Whelan et al. (13) had described previously it had been reported that 30% of women in North America who have breast conserving surgery do not have whole breast irradiation afterwards due to reasons such as inconvenience and cost. According to radiobiological models, hypofractionation in accelerated therapy may prove just as effective as the conventional fractionation schedule. This is also more convenient and uses fewer resources. The group compared whole breast irradiation that was given a total of 50 Gy in 25 fractions over five weeks with a total of 40-44 Gy in 15-16 fractions over 3 weeks. The patients in this study were all treated for invasive carcinoma with negative axillary nodes by breast conserving surgery and axillary dissection. There were also no boosts given to the tumor bed. The patients were seen every 6 months for 5 years and then annually after that. A mammography was done 6 months after radiation therapy and then annually afterwards. Late toxic effects and cosmetic outcomes were evaluated at 3, 5 and 10 years after. The cumulative incidence of recurrence was similar between the two groups (6.7 and 6.2%). However, the hypofractionated scheme seemed to be less effective in higher grade tumors with a difference of about 10% between the two in cumulative incidence of local recurrence. There was no significant difference between the deaths between the two groups. There were also no significant differences in cosmetic outcome at baseline, 5 and 10 years (13).

Other trials in the UK was similarly conducted, the UK Standardisation of Breast Radiotherapy (START) trials A and B compared patients that were treated with 50 Gy in 25 fractions with 41.6 Gy or 39 Gy in 13 fractions and 40 Gy in 15 fractions respectively. Haviland et al.(14) reported the 10 year follow up results

of the START trials. START A results did not show a significant difference between 50 Gy and 41.6 Gy or 50 Gy and 39 Gy for rates of local-regional relapse. It was also reported that there were less normal tissue effects such as breast induration and edema in both 41.6 and 39 Gy groups. START B 10 year follow up results were not significantly different between the percentage of patients that had local-regional relapse between the 50 Gy and 40 Gy groups. Similarly to START A, normal tissue effects were less prevalent in the 40 Gy group (14).

1.8 Dosimetric Effect of Prone Breast Immobilization Device

Immobilization devices are external equipment that are designed to help position patients accurately for treatment delivery. It also assists in the reproducibility of the treatment position throughout the course of a radiation treatment. The overall net dosimetric effect of immobilization devices consists of a changed dose distribution which includes increased skin dose and reduced target coverage. External structures can act as attenuators, scatterers and bolus. Such effects not only apply to the immobilization devices but also to the treatment couch top. During the treatment planning process, these external structures are not always taken into consideration. The American Association of Physics of Medicine (AAPM) Task Group (TG) 176 report summarizes numerous studies conducted on various commercial products and their dosimetric effects, which frequently are clinically significant (15).

The motivations of this dissertation were to study the dosimetric impact of the positioning device and couch systems involved in prone breast radiation at our institution that were not incorporated into treatment plans. It consists of the ClearVue™ prone breast board (Qfix, Avondale, PA), the Varian Exact and Varian Exact IGRT Couch tops (Varian Medical Systems Inc., Palo Alto, CA). The aims of this work can be grouped into three main topics. First, is to quantify the dosimetric effects, i.e. the attenuation and shallow depth (skin) dose effects, of both the immobilization board and couch structures. Second is to

determine the clinical significance of these results. With this, clinical implementation of what can be done to address concerns regarding patient treatment. Furthermore, a Monte Carlo study will be carried out to characterize effects that may not be shown in the commercial treatment planning system with current dose calculation algorithms employed.

Chapter 2: Dosimetric Study

2.1 Introduction

Historically, treatment planning systems did not have the capability to incorporate couch structures as well as immobilization devices into the treatment plans for dose computation. In the past, when a significant portion of an immobilization board was detected to be within the treatment path, a simple board transmission factor (TF) would be applied to correct the calculated monitor units (MU) of the radiation beam. The AAPM TG 176 was charged to collect data for dosimetric effects caused by these external structures and published their report in 2014. According to the task group's recommendation, external structures that are present during treatment delivery should be taken into consideration. Accounting for frequently what is clinically significant will ensure sufficient dose to the treatment target. Several studies are referenced (15) showing different couch tops used in radiation therapy that can attenuate up to 17% and a wide range of patient accessories or immobilization devices that cause a large increase in surface dose, typically an additional 30-50% compared to reference fields, with some cases of more than that. It is of interest to determine this for the products that were present in prone breast radiation.

At our institution, patients are treated with the ClearVue prone breast board, a platform that is used to immobilize and position the breast for more accurate treatment delivery. Traditionally, the external immobilization device and couch structures are not taken into consideration during the treatment planning process. However, with the use of prone tangential beam geometry, there is the possibility of the medial beam intersecting with the prone breast board, couch top and couch rail structures. Couch structures can consist of higher density material, resulting in significant attenuation of the beam. Furthermore, with the board structures present in the beam, there is a concern of potential additional scatter material that may contribute to a higher patient skin dose. In this chapter, the dosimetric effects

(i.e. attenuation, scatter and bolus effects) of these couch top and prone breast board structures will be quantified through phantom studies.

2.2. Materials and Methods

2.2.1 Prone Breast Board and Treatment Couch Systems

The ClearVue breast board is a two-level platform which consists of a carbon fiber board base and an elevated upper level on which the patient lies (Figure 2-1A and 2-1B) (37). The board base structure consists of two layers of carbon fiber sandwiching hard foam. There is a removable insert (Figure 2-1B and 2-1C) as well as handle bars, which aid in reproducible positioning of breast tissue. Figure 2-1C shows the back view of the irregularly shaped insert. The upper level is covered with a urethane/synthetic vinyl/rubber coated cushion for increased patient comfort (37). The breast board can be indexed to existing computed tomography (CT) simulation and treatment couches.

The two clinical couch systems included in this study were the Exact Couch with the Unipanel and the Exact IGRT Couch (Figure 2-2). The Unipanel is a tennis-stringed couch top insert for the Exact Couch top (Figure 2-2A). Below this panel are two moveable carbon structural rails that can be set in two positions (16) , i.e. “in” and “out” (Figure 2-3). Varying rail positions allow more gantry angle possibilities during treatment planning as well as clearer anterior-posterior imaging without overlaying rails. The rails are “in” when both are pushed towards each other with the smallest distance between the two. The rails are “out” when they are pulled away from each other with the maximum distance possible between the two. The Exact IGRT couch (Figure 2-2B and 2-2C) consists of a carbon fiber shell with hard foam inside.

In contrast to the Exact couch, it does not have couch rails and the couch top thickness varies along the longitudinal direction.

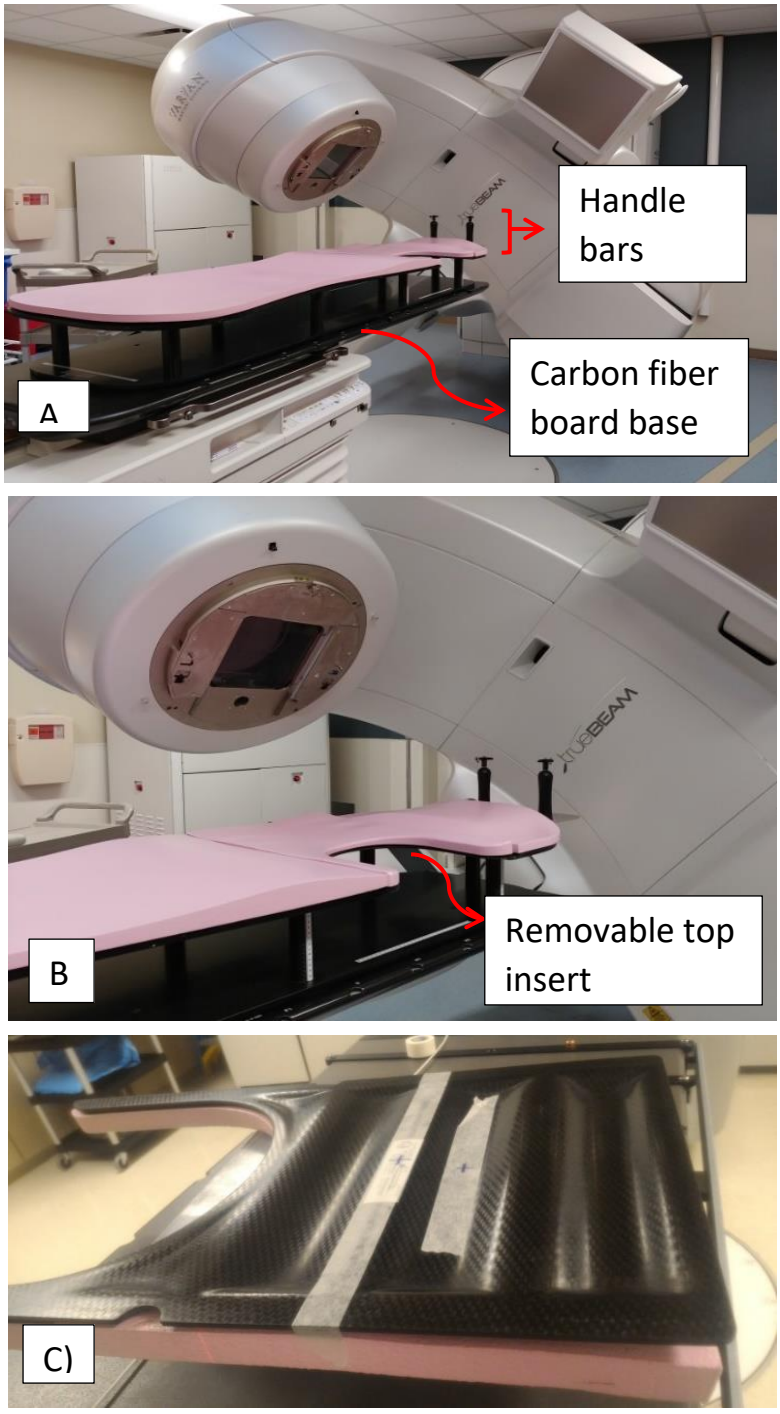

Figure 2-1: Clearvue™ prone breast board. A) Full view of breast board showing handle bars and board base, B) Close up image of the removable top insert on the board, C) Irregular shape of insert.

Figure 2-2: Varian couch systems. A) Exact Couch with tennis-stringed couch top insert and moveable couch rails, B) Exact IGRT Couch, C) Variable thickness along the longitudinal direction of the Exact IGRT Couch.

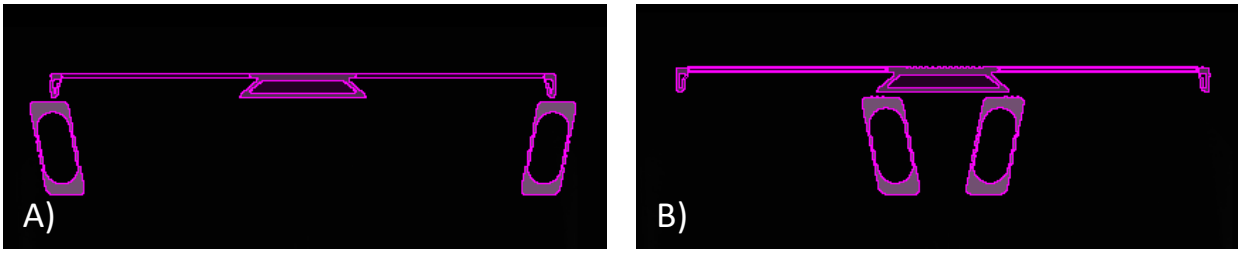

Figure 2-3: Structure of Exact Couch model in the treatment planning system. A) Couch rail position “out”, B) Couch rail position “in”.

2.2.2 Measurement of Transmission Factors

The attenuation effect can be characterized by the measurement of transmission factor (TF). The TF is given by equation (1):

$$TF = \frac{Rdg\ with\ object\ of\ interest}{Rdg\ without\ object\ of\ interest} \text{ at depth} > d_{max} \quad (1)$$

TFs of the board base and removable top insert of the ClearVue prone breast board were measured. A schematic of the general setup is shown in Figure 2-4A. A 0.6cc cylindrical Farmer Chamber (Model N30013, PTW, Germany) was placed at a depth of 4 cm in a Lucite phantom. Measurements were taken with a 100 cm source to chamber distance (SCD), 10x10 cm^2 field size, 100 monitor units (MUs) and with gantry angles 0-40° in 10° increments.

TFs of both the Exact Couch and Exact IGRT Couch were measured using a geometry that was recommended by the AAPM TG176 report (15) as seen in Figure 2-4B. A cylindrical acrylic phantom with a 19 cm diameter was centered on both couch tops. For the Exact Couch, we took measurements with the rails in both the "out" and "in" positions. A 0.125cc thimble chamber (Model 31010, PTW, Germany) at the center of the phantom was placed at isocenter (SCD = 100 cm). The field size was 10x10 cm^2 and 200 MUs were delivered. We normalized readings to 270 degrees where the beam was unobstructed. All TF measurements were then repeated on another day for a reproducibility check.

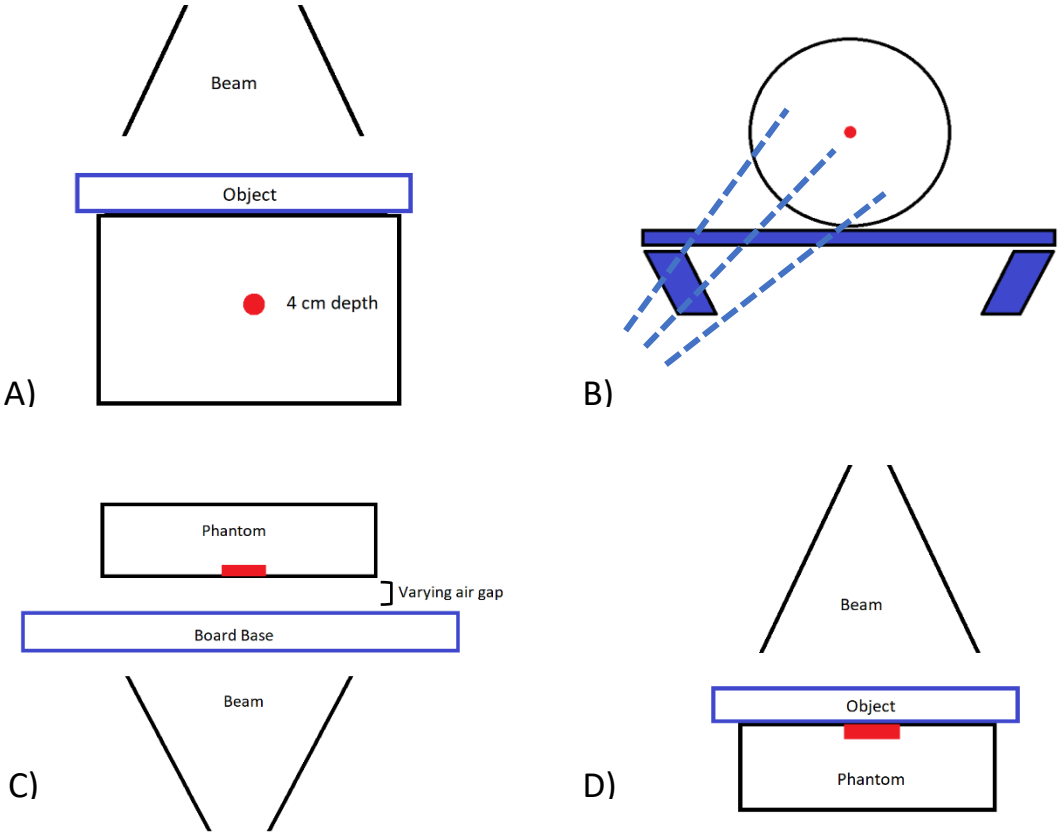

Figure 2-4: Schematics of experimental setups. A) Measurement setup of transmission factors with a farmer chamber placed at 4cm depth, B) Couch attenuation setup a thimble chamber centered in a cylindrical phantom which is centered on the couch top, C) Scatter effect setup with parallel plate chamber at phantom surface facing the board base with varying air gaps with gantry angles starting at 180 degrees, D) Bolus effect setup with parallel plate chamber at phantom surface with gantry angles starting at 0 degrees. Locations of chambers are in red.

2.2.3 Board Scatter and Bolus Effects

We performed initial shallow depth dose measurements to demonstrate the effect of scatter from the board base and bolus effect from the top insert. The setup in Figure 2-4C consisted of a Markus Parallel Plate Chamber (Model 23343, PTW, Germany), with the 1 mm build up cap, placed at the surface of a 5 cm phantom block facing the board base. The SCD was 100 cm and a 10 x 10 cm^2 field size was used. Readings were taken with various air gaps between the surface of the phantom and the board base (0 to

10 cm) at gantry angles of 180-220° in 10° increments with 100 MUs delivered. We normalized readings to the largest air gap of 10 cm to show the relative increase of dose at 1 mm depth as a function of decreasing air gap (i.e. increasing breast size) as well as with gantry angle. To study the bolus effect from the top insert, a "bolus ratio" was determined with the following equation:

$$Bolus\ Ratio = \frac{Rdg\ with\ object\ of\ interest}{Rdg\ without\ object\ of\ interest} \text{ at shallow depth} \quad (2)$$

A Markus parallel plate chamber with a 1 mm build-up cap was placed at a SCD of 100 cm at the surface of a phantom with the top insert situated above (Figure 2-4D). Measurements were taken with 100 MUs delivered at gantry angles of 0-40° in 10° increments with a 10 x 10 cm^2 field size.

Further measurements were done to investigate scatter effects with depth. A scatter ratio was also calculated following equation (3):

$$Scatter\ Ratio: \frac{Scatter\ measurement\ rdg\ (air\ gap, depth)}{No\ scatter\ reference\ dmax\ rdg} \quad (3)$$

For this calculation two setups were involved, a reference "no scatter" setup (Figure 2-5) and the other setup shown in Figure 2-4C with the board (i.e. additional scatter material). The "no scatter" setup consists of the standard geometry (Source to surface distance, SSD= 100 cm, 10x10 cm^2 field size, 100 MU) without the board base present. The setup in 2-4C was used with a few differences: the build up cap was removed and solid water slabs were used to add depth. By normalizing to the maximum reading from the "no scatter" setup, this takes into account that there is also scatter contribution with a 10 cm air gap. Measurements were taken up to a 2 cm depth for various air gaps (0-10 cm).

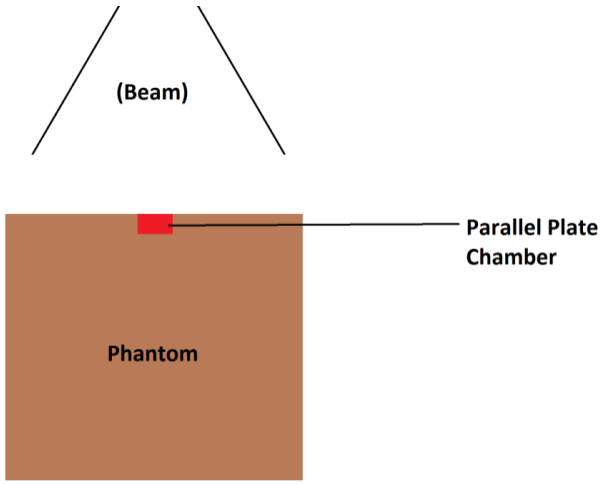

Figure 2-5: Illustration of the "no scatter" setup for scatter depth dose measurements.

2.2.4 Treatment Planning System (TPS) Verification of Transmission Factors

To verify the experimental TF results in the TPS, treatment plans were created in the Eclipse™ TPS (Version 15.6, Varian Medical Systems Inc., Palo Alto, CA) using the CT image of the breast board to mimic the experimental measurement setups. A phantom block was created in the treatment plan with either the board base or insert included into the body contour. A separate plan was created with just the phantom. By including structures into the body contour, all original CT Hounsfield Units (HUs) can be taken into account. A reference point at 4 cm was created and the phantom was assigned a HU of 120 to approximate the Lucite phantom. The TFs were obtained by using the same formula as in equation (1) by taking the ratio of the doses at the reference point in each plan. Similarly, a default model of the Exact Couch top with the rails in the "out" and "in" position was added to plan with a CT image of the acrylic phantom with assigned HU of 120 (Figure 2-4B). A reference point was placed in the center of the phantom. For the Exact IGRT Couch, the couch top with medium thickness was selected. Doses recorded for the reference point were normalized to that of gantry angle 270.

2.3. Results and Discussion

2.3.1 Prone Breast Board Transmission Factors

Table 2-1 shows the TFs for the top insert. Overall, at larger gantry angles (e.g. 220 degrees), the TF is lower. The range of the TFs appears to be larger for readings taken at the crest of the insert. This is due to the irregular shape of the insert (Figure 2-1C). For 6 MV, the TFs were 0.976-0.983 for the crest and 0.978-0.980 for the trough. For 23MV, values ranged from 0.990-0.999 for the crest and 0.992-0.999 for the trough. Values obtained from the TPS were in agreement within 0.6%. Table 2-2 shows the TFs for the board base. Values ranged from 0.979-0.985 and 0.989-0.998 for 6 and 23 MV respectively for the base of the board. Overall, TFs decrease with increasing gantry angles. TPS values agreed within 0.4%.

The attenuation of the insert does vary depending on which portion which is in the beam. Results in Table 2-1 show TFs of portions of the insert that will not be in the beam. The concern of the insert will mostly be the enhancement of the surface dose. The attenuation of the board base will depend on gantry angle and is also combined with the attenuation of the couch top.

Table 1-1: Top insert transmission factors for 6 and 23 MV

6 MV	(Centered on Crest)				(Centered on Trough)		
*Angle (°)	Eclipse	Measured	% difference	*Angle (°)	Eclipse	Measured	% difference
180	0.982	0.983	0.0	180	0.981	0.980	0.1
190	0.982	0.980	0.2	190	0.982	0.981	0.1
200	0.976	0.973	0.4	200	0.982	0.982	0.0
210	0.971	0.972	0.1	210	0.983	0.982	0.1
220	0.974	0.976	0.2	220	0.978	0.978	0.0
23 MV	(Centered on Crest)				(Centered on Trough)		
*Angle (°)	Eclipse	Measured	% difference	*Angle (°)	Eclipse	Measured	% difference
180	0.993	0.999	0.6	180	0.992	0.999	0.6
190	0.993	0.999	0.6	190	0.993	0.999	0.6
200	0.989	0.993	0.4	200	0.992	0.998	0.5
210	0.985	0.990	0.6	210	0.992	0.996	0.4
220	0.985	0.990	0.5	220	0.988	0.992	0.4

*equivalent angle in the range 180-220 degrees when gantry angles 0-40 degrees were used

Table 2-2: Board base transmission factors for 6 and 23 MV

6 MV				23 MV			
*Angle (°)	Eclipse	Measured	% difference	*Angle (°)	Eclipse	Measured	% difference
180	0.988	0.985	0.3	180	0.996	0.998	0.2
190	0.988	0.984	0.4	190	0.996	0.997	0.1
200	0.988	0.984	0.4	200	0.995	0.996	0.2
210	0.986	0.982	0.4	210	0.993	0.993	0.1
220	0.983	0.979	0.4	220	0.991	0.989	0.1

* equivalent angle in the range 180-220 degrees when gantry angles 0-40 degrees were used

2.3.2 Couch Structures Transmission Factors

Figure 2-6 displays the TFs measured for the Exact Couch at selected angles at two couch rail positions, "out" and "in". TFs ranged from 0.836 to 1 for rails "out". There are two dips in the curve where TFs are at a minimum with a local maximum in between. When the rails were "in", TFs were 0.838-1. Similarly, there are a series of dips where the TFs are a minimum with local maximum in between. Both TF curves also show a slight dip at a gantry angle of 245°. TFs obtained from the TPS follow a similar trend with a 5-8% difference in areas of maximum attenuation. The trend of TF measurements was reproducible at a separate day. The maximum percentage difference of these TFs was determined to be 0.9% and 3.2% for the Exact Couch with rails "out" and Exact Couch with rails "in". The average percentage difference was within 0.5% for both. The higher percentage difference for the Exact Couch when rails "in" could be due to setup error such as misalignment of the cylindrical phantom between the two sets.

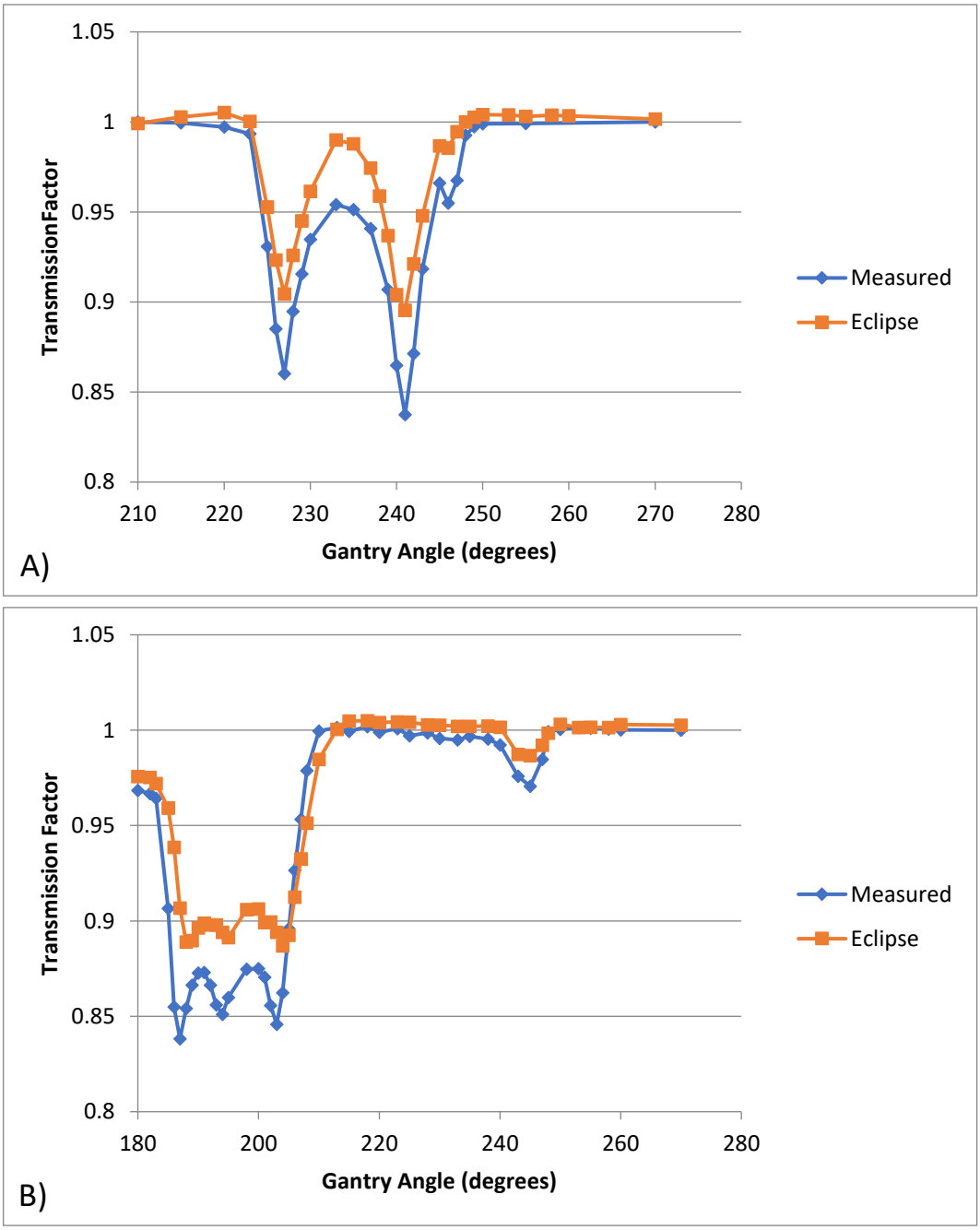

Figure 2-6: Transmission factor curves for Exact Couch for 6 MV. A) Couch rail position is "out", B) Couch rail position is "in".

Figure 2-7 shows the TFs of the Exact IGRT Couch top. The TFs decreases slowly to 0.956 as the beam approaches where the largest path of material at a gantry angle of 248°. Afterwards, values increase gradually towards a gantry angle of 270°. The TPS curve follows a similar trend with up to 2.5% difference at areas of maximum attenuation. The TF measurement results were reproducible at a separate day. The maximum percent difference of these TFs was determined to be 1.7% with an average percentage difference of 0.3%.

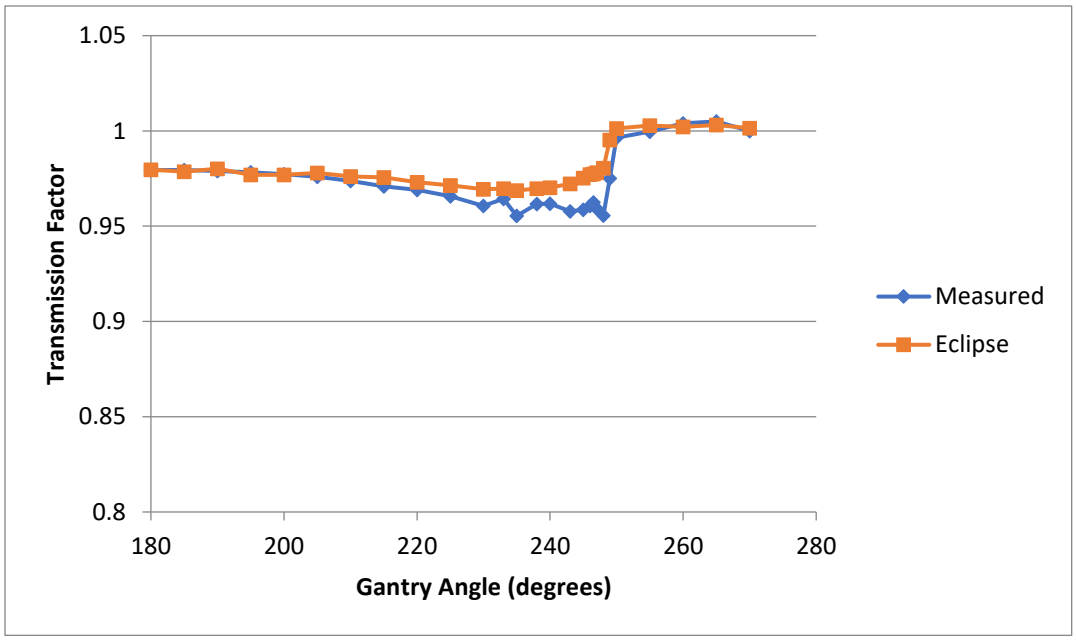

Figure 2-7: Transmission factor curves for Exact IGRT Couch for 6 MV.

While both the immobilization board and couch structures attenuate the beam, the couch structures can attenuate the beam much more. Results from 2.3.1-2.3.2 are similar to those of TG 176 (15). The attenuation from the Exact Couch can be up to 16%. This may lead to a reduction of the dose delivered to the target in patients depending where the beam crosses through the couch rails before reaching the patient and where the clinical treatment volume is located. This could also affect local control. For the Exact IGRT couch, there is less attenuation and variation with gantry angle. Discrepancies between measured and TPS values may also be due to positioning and assigned HUs to different components of

the TPS model. A past study conducted by Wagner and Vorwerk (16) looked at the modeling of the Exact Couch with the flat panel in the Eclipse TPS. They found that dose differences ranged from -3.6 to 8.4% between measurements and calculations when using default couch structure values in the TPS. Additionally, the model in Eclipse TPS does not take into account denser edges on the Exact IGRT Couch which are revealed in a cone beam CT image.

2.3.3 Breast Board Scatter and Bolus Effects

As seen in initial scatter measurement results (Figure 2-8), when in close proximity (a few centimeters) of the board base, there is a relative increase of skin dose (measured at 1mm depth) to at least 23% compared to a 10 cm air gap for 6 MV. Similarly, for 23MV, there is at least a 25% increase with close contact. The relative increase is more linear from 10 cm to 4 cm in both figures and plateaus afterwards. Curves follow a similar trend for different gantry angles but the difference is small between them. Measured experimental results for the bolus effect in Figure 2-9 show that the insert increased the dose at 1 mm depth by 65-93% for 6 MV and 117-157% for 23 MV. This effect decreases slightly with gantry angle.

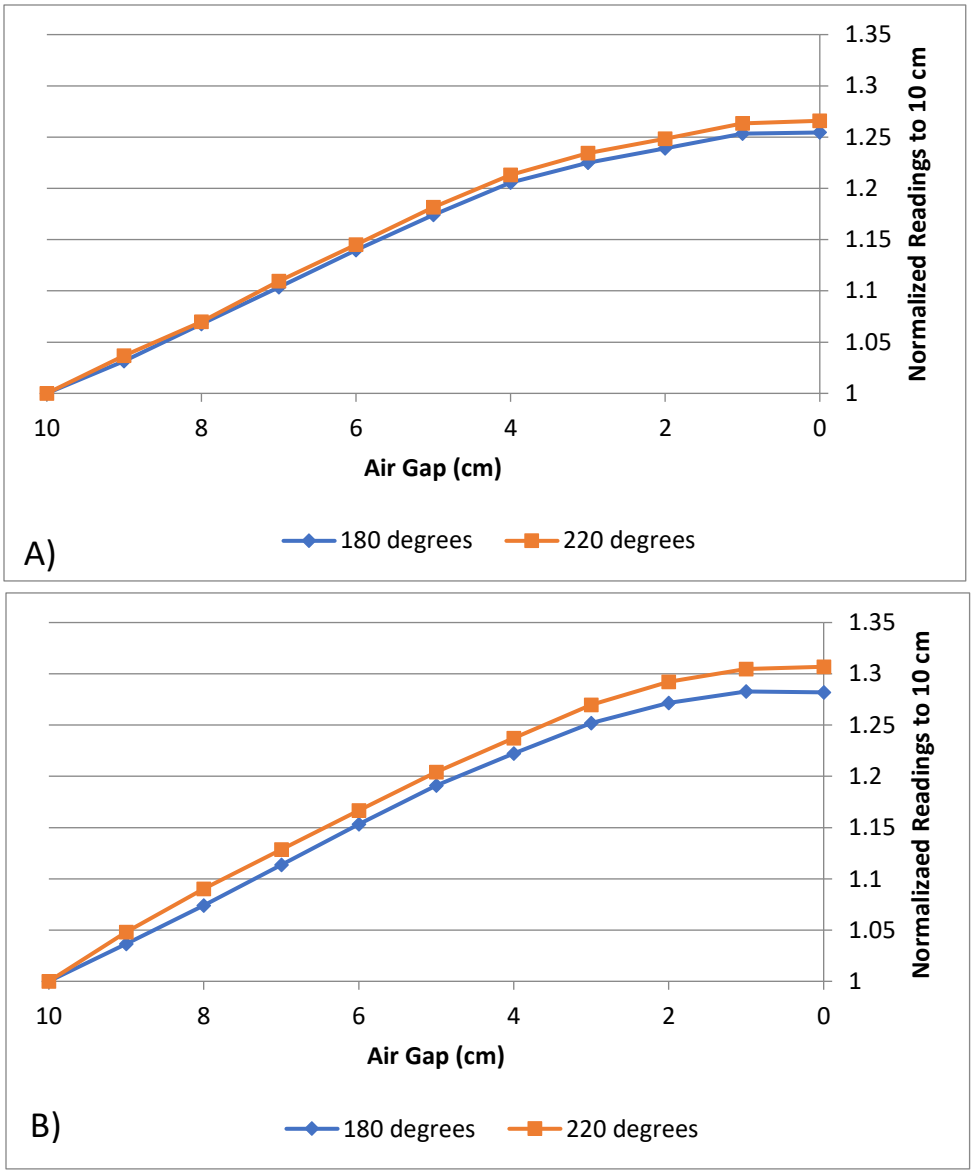

Figure 2-8: Scatter contribution from board base. Readings normalized to the 10cm air gap. Gantry angles of 180 and 220 degrees are shown. A) 6 MV, B) 23 MV.

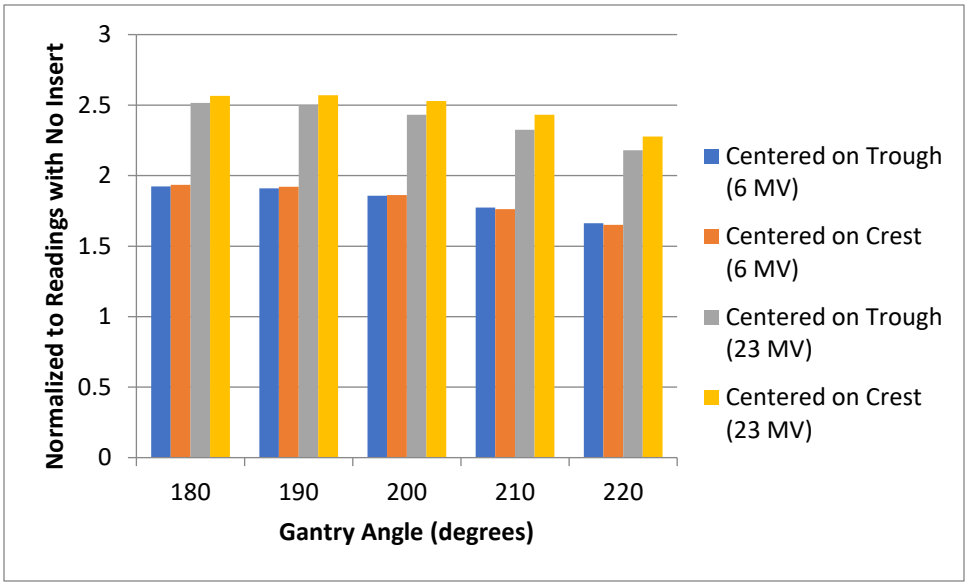

Figure 2-9: Bolus effect results from top insert. *note: equivalent angles 180-220 degrees were used in graph.

The trend that is seen in Figure 2-8 demonstrates the effect of an air gap has on surface doses. With a larger air gap, the lateral spread of electrons from additional scatter material can reduce the surface dose. A study which was referenced in TG 176 conducted by Gray *et al.* also show this effect when they looked into the accuracy of TPS algorithms when immobilization and large air gaps were involved (11). When air gaps greater than 5 cm were introduced, the surface dose would be greatly reduced compared to smaller air gaps. Becker *et al.* (17) conducted a study looking at the impact of two different breast positioning systems on potential skin dose reactions. They compared two pad materials: foam with a nylon cover and a helium-filled Mylar bag. Their results showed that when the distance between the foam pad and phantom was decreased, the surface dose was increased by up to 3 times of that when no pad was present. Also, by taking build up measurements, they found that the percent depth dose (PDD) curve of a separation/air gap of 2 cm between the foam pad and phantom was similar to the PDD curve of a phantom having a 2.5 mm bolus. Our results in Figure 2-8 follow the same trend that is seen the study done by both works mentioned previously. Patients with a smaller air gap, or none at all, could experience an increase in surface dose to the apex of the breast depending on the gantry angle. Also, if

swelling occurs from treatments, this could also reduce the air gap. To minimize dose to the skin, the breast could be elevated to a larger distance from the breast board. This however may create more skin folds and there may be inconsistencies with the shape of the breast that is being treated. The ClearVue breast board is available in two height options, 17.5 and 20 cm, in which the board with increased height may increase the air gap between the breast and the board. However, with increased height, it is limited by the possibility of collision with the gantry head.

Measured results further show an increase to the surface dose with contact to the insert. Potential clinical implications could visible skin reactions in areas where the insert is in the treatment field such as the mediastinum and skin superior to the breast. To reduce skin dose, it would be important to reduce the portion of the insert in the field if possible. This could be done by using an insert with a larger aperture size when applicable. One should be cautious, however, when selecting a larger aperture as it may affect patient stability during treatment positioning.

Figure 2-10 show scatter measurement values which are normalized to the corresponding “no scatter” reference reading at each depth (Figure 2-5) for the air gaps of 0, 5 and 10 cm. At depths greater than 0.8, the effect of the air gap was minimal and all curves look similar. The effect of the air gap has the most effect on the surface readings (Figure 2-11). If a ratio is taken with board to no board (“no scatter” reference) at 0 cm, it ranges from 1.9 to 3.2 across all air gaps.

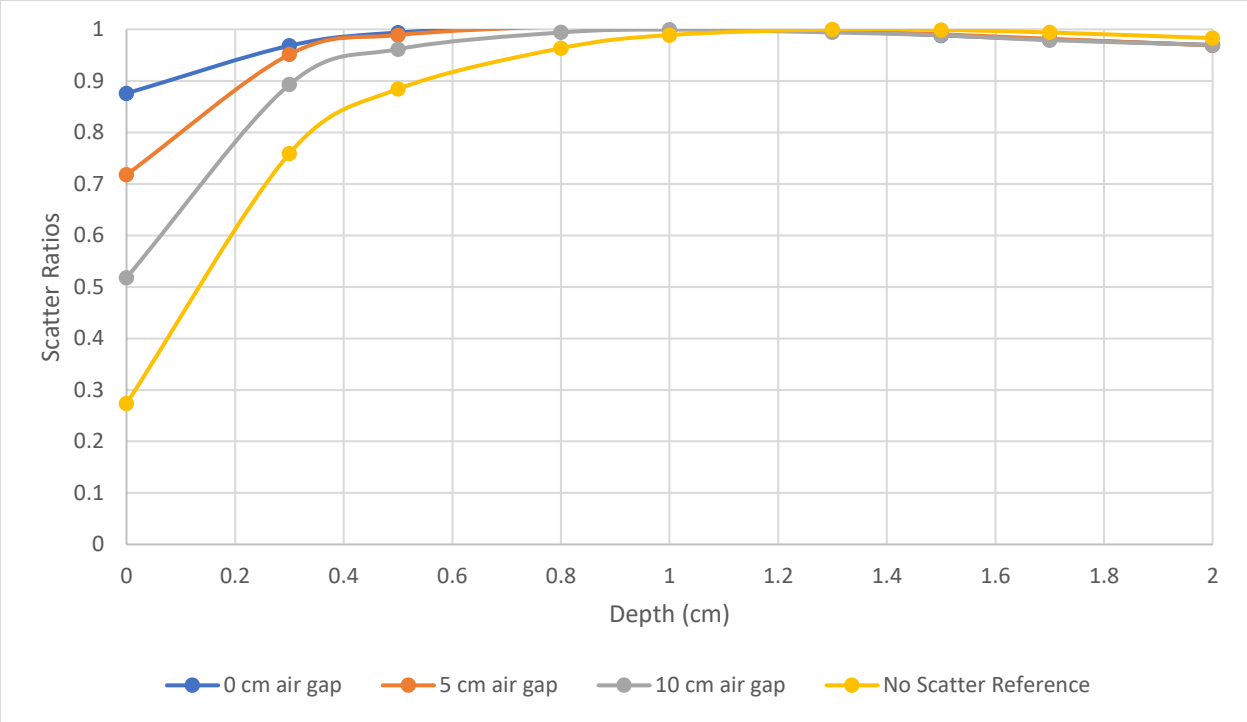

Figure 2-10: Scatter ratios as a function of air gap for selected depths. The reference curve is shown in yellow for comparison.

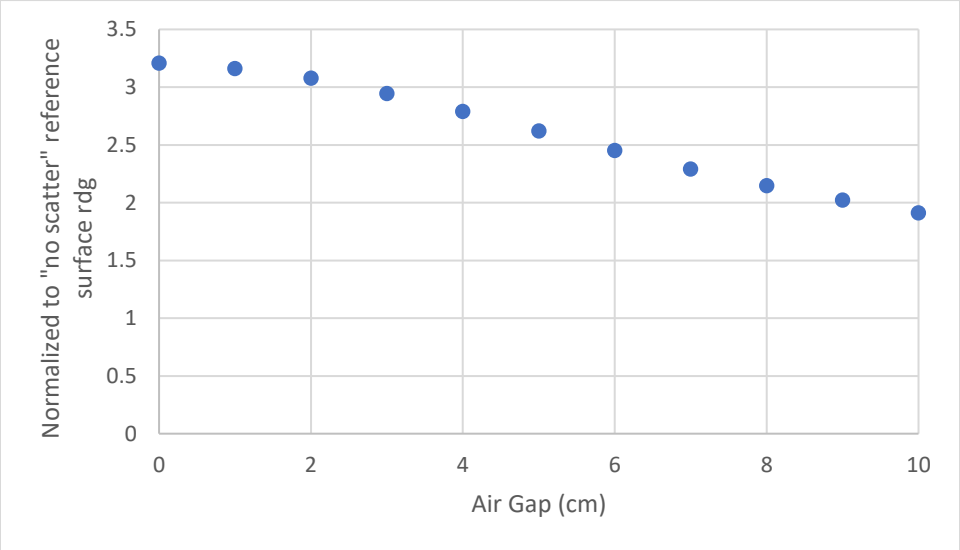

Figure 2-11: Scatter ratios normalized to the “no scatter” reference setup for the depth of 0cm as a function of air gap.

2.4. Summary

Results of this chapter show that the immobilization board and couch structures do attenuate the beam and this leads to clinical concerns of decreased target dose. Increased surface doses are seen with smaller air gaps with the board base and contact with the insert. Chapter 3 continues to explore the clinical significance of these results. The AAPM Task Group 176 report recommends to take into account the dosimetric effects such as avoiding treatment plans that involve beams that go through these external devices (15). Using available couch models and other tools available in the TPS, one may determine where the beam may intersect with the couch and can choose an alternative gantry angle. This may be difficult in prone breast cases due to tangential field geometry and variation of patient breast size. Therefore, it would be important to be able to model the breast board and have these external structures taken into consideration during dose calculation.

Chapter 3: Clinical Significance and Implementation of a Custom Model

3.1 Introduction

Results shown in the dosimetric study in Chapter 2 demonstrate that there is a measurable effect from the attenuation of components of both the immobilization board and the couch top. Since traditionally neither of these structures are included in the treatment planning process, it is important to investigate the significance of general phantom study results in a more clinically relevant setting. which includes typical treatment gantry angles, field sizes and various patient characteristics. With prone breast radiation, opposed tangential photon beams are used (i.e. medial and lateral). Of the two, only the medial beam could traverse through not only the couch top but also the prone breast board, potentially affecting the dose delivered to the patient. In this chapter, we will look at a sample of the patient pool to demonstrate the clinical significance of previous results.

At our institution, standard prone breast treatment plans are developed utilizing the electronic tissue compensation (ECOMP) technique. The ECOMP treatment planning technique generates an optimal fluence using dynamic multi-leaf collimators (dMLC) to deliver a more homogeneous dose distribution to irregular surfaces (18). The treatment planning software creates a dose profile using beamlets in the field, which is then converted to an intensity profile that allows delivery of a homogenous dose to a user defined depth in tissue (19). This is described as the tissue penetration depth (TPD) and is a percentage of the total distance of tissue that the beamlet travels through (19). Differences in the tissue in the superior-inferior and anterior-posterior directions are taken into account through this technique (19).

3.2 Materials & Methods

3.2.1 Patient Data

We retrospectively collected the treatment plan data of the first 44 prone breast patients that were treated at our institution from the Eclipse TPS. This included patient characteristics and treatment setup parameters such as the following: prescription doses, breast size, breast length, breast width, gantry angle and isocenter location. Prescribed doses range from 40-50 Gy with fractional doses of 1.8-2.67 Gy/fx. Breast size was represented by the air gap between the apex of the breast and board base shown in Figure 3-1A. Breast dimensions are described as in Figure 3-1B. A summary of patient characteristics is given in Table 3-1.

Table 3-1: Summary of patient characteristics

Summary Table of Patient Characteristics	
Number of patients	44
Breast lengths	4.4 - 21.4 cm
Air gaps	0.8 - 13.8 cm
Medial field gantry angles	232-264(right breast treatments) 95-120 (left breast treatments)
Fractional doses	1.8 – 2.67 Gy/fx
Total prescription doses	40 – 50 Gy (additional boost may follow)
Breast Size Groups	
Small (air gap ≥ 9 cm)	11
Medium (6 cm ≤ air gap < 9 cm)	16
Large (2 cm ≤ air gap < 6 cm)	11
Very large (air gap < 2 cm)	4
Pendulous (lying on Styrofoam) (Figure 4C)	2

Patients were grouped into multiple size categories based on the air gap measured. For patients who had 'pendulous' breasts where breast tissue would rest on the board base, a Styrofoam™ (approximately 2cm thickness) was used for reproducible positioning of the breast during treatment delivery (Figure 3-1C). The possibility of the medial beam passing through the couch top and rail structures was also evaluated in the TPS. This was carried out visually in individual patient plans after inserting the Exact Couch model. There were 31 out of 44 patient plans in which the medial treatment beam passed through the rails when in the "out" position and 15 out of 44 patient plans in which the same occurred when the rails were "in".

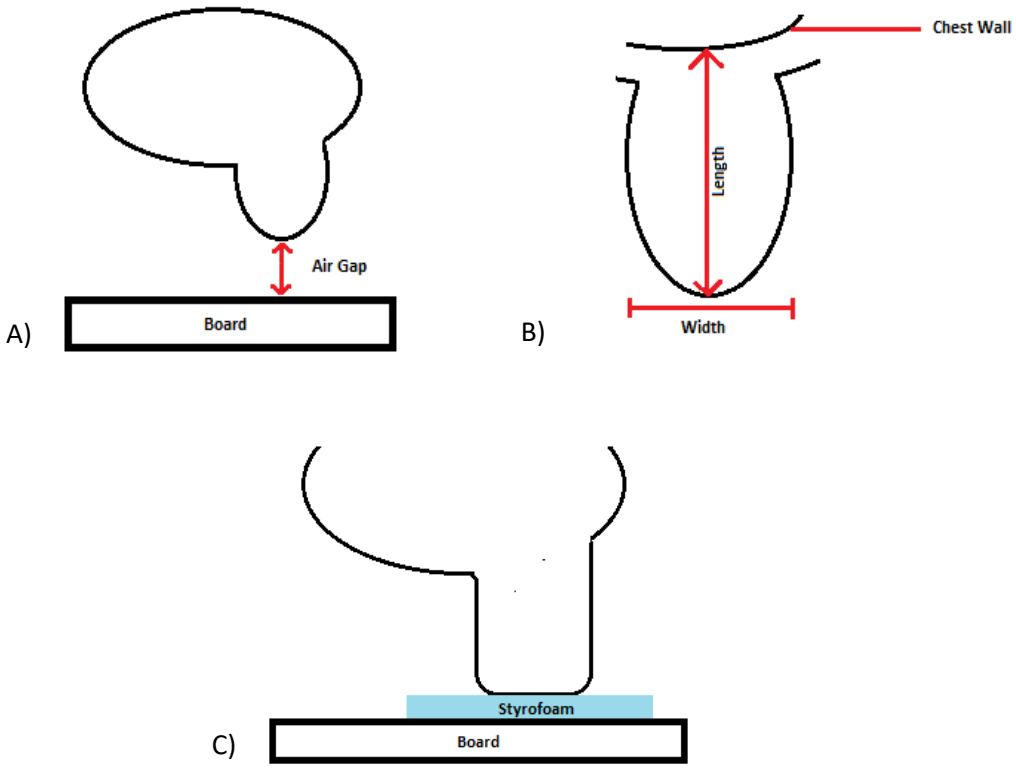

Figure 3-1: Definition of patient characteristics. A) Definition of air gap, B) Definitions of breast length and width, C) Largest breast size demonstrated where breast rests on Styrofoam during treatment.

3.2.2 Effect of Breast Board and Couch Structures on Target Coverage in Clinical Cases

We chose four scenarios to demonstrate how target coverage is affected when the medial beam passes through the Varian Exact Couch structures. Figure 3-2 shows the beam's eye view of each scenario where the structures in pink are the couch top and structures in dark blue are the couch rails. Firstly, we looked at a group of patients whose treatment plans had any part of the treatment beam passing through the couch top or rails while in the "out" position. Scenarios were then based on an "in" couch rail position criterion for that group, the "rails in" criterion. The treatment field typically includes the treated breast with a margin (skin flash). The four categories were maximum blockage, moderate blockage, slight blockage and very little or no blockage of the treatment field. Maximum blockage (Figure 3-2A) describes the situation when the "rails in" criterion is met where part of the breast tissue within the treatment field is blocked by "in" rails. Moderate blockage (Figure 3-2B) describes the "rails in" criterion is met when other attenuating areas of the couch top (e.g. center metal spine of panel) were blocking breast tissue. Slight blockage (Figure 3-2C) describes the "rails in" criterion is met when less attenuating areas (e.g. tennis stringed portion of panel) were within the treatment field. Very little or no blockage (Figure 3-2D) describes the "rails in" criterion is met when only small areas of the couch top panel edge were within the treatment field. We then selected 2 patients from the patient pool that satisfied each scenario.

For each patient, we created three additional plans in Eclipse TPS which incorporated the prone breast board and couch structures collectively: breast board and Exact Couch with rails "out", breast board and Exact Couch with rails "in" and breast board and Exact IGRT Couch with the medium thickness option. In these plans, the same treatment field parameters as the original clinical plan (e.g. field sizes, gantry angles, dMLC fluences, and MUs) were used to compute the dose coverage to both the clinical treatment volume (CTV) and the whole breast (WB) for comparison with the original intended coverage.

From each plan, we recorded the percentage volume of the CTV that received 95% of the prescription dose (CTV V_{95}), and used it to evaluate target coverage. A WB contour was created and 3 mm was subtracted to account for the skin sparing effect when using megavoltage beams. Similarly, the volume that received 95% of the prescription dose (V_{95}) was then recorded to evaluate WB coverage.

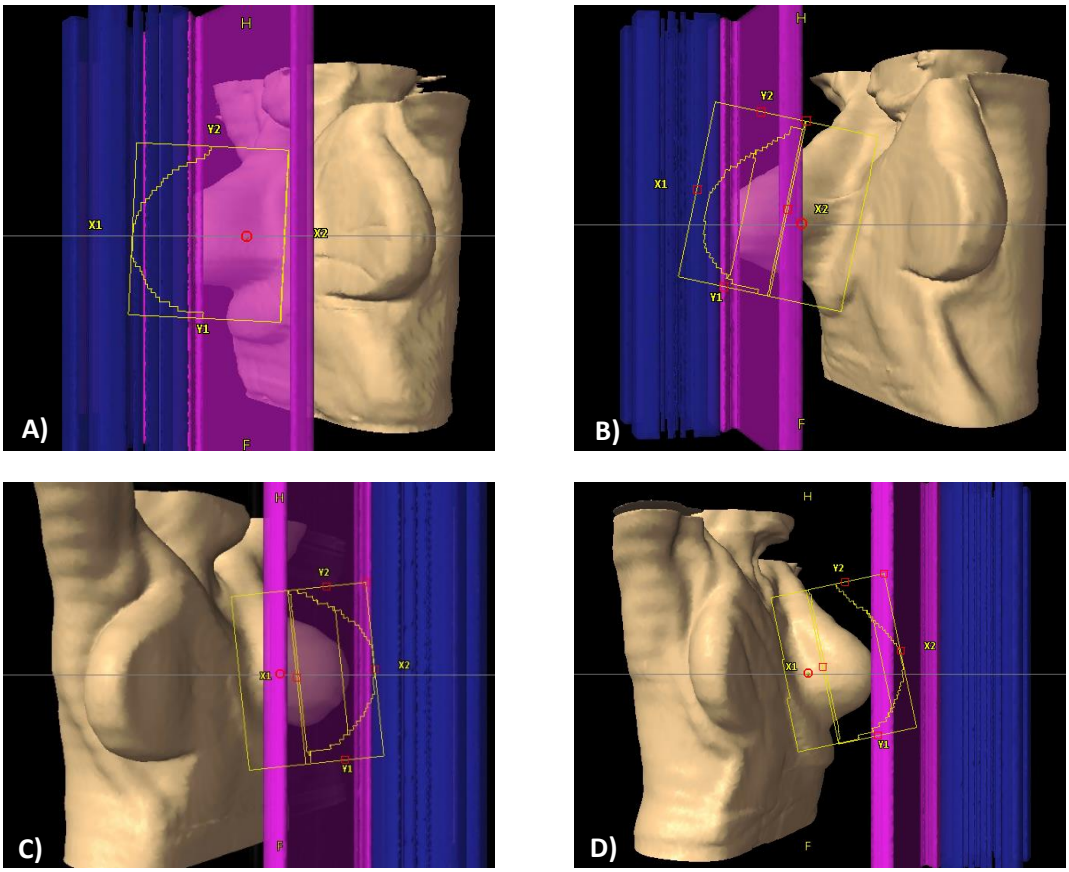

Figure 3-2: Example patients displaying selection criteria for four different scenarios. Rail structures are in blue, couch panel is in purple. A) maximum blockage when rails are "in"; criterion for scenario 1, B) moderate blockage when rails are "in"; criterion for scenario 2, C) slight blockage when rails are "in"; criterion for scenario 3, D) little or no blockage when rails are "in"; criterion for scenario 4.

3.2.3 Implementation of a Custom Prone Breast Board Model

With a variation of treatment gantry angles chosen based on patient specific characteristics such as breast size, it is important to model the breast board in the TPS. For example, a larger breast sizes (i.e. larger field size) may have the beam traversing a larger portion of the board. Tools within the Eclipse TPS

allow the creation of custom support models for more an accurate representation of immobilization devices during the treatment delivery. During the treatment planning process, these models can be added into the treatment plan with ease rather than manually contoured separately for every patient.

Creating a custom model in the Eclipse TPS involves two steps, contouring the structure(s) of interest as 'Support' type and then selecting the command 'Create and Manage Support Structure Models' in the 'Contouring' workspace. There are two types of models that can be created. One involves having the structure(s) of interest contoured in its entirety over multiple slices along the z-axis of the CT image set. The other involves having the structure(s) contoured only on one slice. The former allows creation of a 3D model with variation of thickness along the z-axis, while the latter will create a model which has a uniform thickness. The 'Contouring' workspace is also only the workspace which allows insertion of a custom model into a treatment plan.

The main components of the breast board, i.e. board base and insert, were contoured, set as support structures and the appropriate CT number or Hounsfield Unit (HU) was assigned to each. The HUs were determined by matching the TFs that were obtained from previous experimental results. The board base model consisted of two structures, the 'base shell' and 'base inside'. This represents the composition of the board base which is a layer of hard foam sandwiched between two layers of carbon fiber. Both were combined to make a 3D custom model of the prone breast board.

3.2.4 Treatment Plan Incorporating Immobilization and Couch Structures

To demonstrate the dosimetric impact of patient support structures in clinical prone breast cases, we selected a patient whose target coverage was substantially affected. We incorporated the additional immobilization and couch structures to generate an acceptable clinical treatment plan for comparison. The default model of the Varian Exact Couch in Eclipse TPS was added into the plan. Similarly, the

custom board model was added as well. A new electronic compensation plan was created and the fluence was manually painted to give the desired dose distribution.

3.3 Results & Discussion

3.3.1 Potential Target Under-Coverage

Eight representative patients in the 44 patient cohort were selected to study the potential compromise of target coverage due to attenuation from the external structures. Table 3-2 and Table 3-3 display the CTV V95 and WB V_{95}, the volume of the CTV and WB that receives 95% of the prescription dose. Patients 1 and 2 were selected for scenario 1, patients 3 and 4 were selected for scenario 2, patients 5 and 6 were selected for scenario 3 and patients 7 and 8 were selected for scenario 4, respectively. Plans demonstrating the overall effect of including the immobilization board and couch structures are shown. Out of the 8 patients, CTV coverage of 6 patients was affected when couch rails are "out" for the Exact Couch. Only 1 patient's CTV coverage was affected when the rails were "in". For both patients of scenario 4 (i.e. patients 7 and 8) the CTV coverage was unaffected. The Exact IGRT Couch plans resulted in either small (within 0.2%) or no reduction in target coverage for 5 out of the 6 patients. WB V_{95} values show the most reduction in WB coverage in all 6 patients when using the Exact Couch with rails "out".

Table 3-2: CTV V_{95} for selected patients of the 4 created scenarios.

CTV V_{95}	Patient 1	Patient 2	Patient 3	Patient 4	Patient 5	Patient 6	Patient 7	Patient 8
1)Original	100.0	100.0	100.0	100.0	100.0	100.0	100.0	100.0
2)Breast board and Exact Couch rails "out"	95.8	97.7	94.9	93.4	97.8	85.2	100.0	100.0
3)Breast board and Exact Couch rails "in"	100.0	100.0	97.6	100.0	100.0	100.0	100.0	100.0
4)Breast board and Exact IGRT Couch medium thickness	99.9	100.0	90.9	100.0	99.8	100.0	100.0	100.0

Table 3-3: WB V_{95} for selected patients for the 4 created scenarios.

WB V_{95}	Patient 1	Patient 2	Patient 3	Patient 4	Patient 5	Patient 6	Patient 7	Patient 8
1) Original	94.8	95.5	93.2	90.3	90.2	94.9	88.5	89.5
2) Breast board and Exact Couch rails "out"	80.9	67.9	88.7	72.7	65.5	79.5	87.9	89.6
3) Breast board and Exact Couch rails "in"	87.5	95.2	92.0	85.6	85.8	93.8	88.1	89.7
4) Breast board and Exact IGRT Couch medium thickness	88.9	91.9	89.0	80.1	78.9	91.0	87.4	89.4

During the treatment planning process for a breast plan at our institution, 100% of the CTV must be encompassed by the 95% isodose line. A majority of the patients evaluated for target coverage by using the scenarios created in this study have reduced CTV coverage due to the couch rails being "out". The simple solution is to push the rails in during treatment. The Exact Couch with rails "out" compromised WB coverage the most, followed by the Exact IGRT Couch and then the Exact Couch with rails "in". Values in Table 3-3 show that even if the CTV coverage is not affected (i.e. cases with rails "in" and the IGRT couch), WB coverage is still affected. This is still not ideal since the WB is the target of prone breast radiation. Although these patients were selected by criteria which were based on the Exact Couch, Patient 3 demonstrates the possibility that even when the Exact IGRT couch is used, coverage can be affected significantly as well. However, the Exact IGRT couch is still recommended for use because it causes less attenuation than the Exact Couch. While the main cause of target coverage reduction is the couch top, the breast board also has the potential to cause a reduction in target coverage. Results of a plan which only included the board base as an external structure (was not shown in table above), the CTV V_{95} was reduced to 98.5. The overall effect that these external structures have on the doses delivered to the breast will depend on several factors such as gantry angle, breast size, shape of the CTV and location of the CTV in the breast relative to the couch or breast board. Beam weighting can be a factor as well. From previous results, one can see that the great variation in TFs is caused by the structure of the couch rail and the edge of the couch top insert. Therefore, the amount of attenuation is dependent on the angle of intersection of the beam and the rail. Results of this section show how target coverage can be comprised when the board and couch are not taken into account. This reinforces the need to have models of both in the TPS to be incorporated into treatment plans.

The combination of breast board and couch top used can also change the extent of this effect on target coverage. Yoo *et al.* (20) presented their findings of the dosimetric effect of a prone breast board by recalculating prone breast treatment plans for 14 patients, each with 3 plans comprised of one plan

which included original CT numbers of the board, another with an assigned CT number for the board and the last with added couch structures of the Exact IGRT Couch. In their study, the mean V_{95} among patients was reduced by a maximum of 1 % and the mean V_{100} was reduced by a maximum of 6.2% when original board CT numbers were used. Their results showed that individually, a breast board and couch structure lead to a reduced coverage of the treated breast volume.

3.3.2 Custom Prone Breast Board Model

Figure 3-3 shows the custom model of the breast board with the large cut-out insert which was created in the TPS. A series of board base combinations and insert HUs were tested to find the best agreement with experimental results. TPS TFs obtained for a range of HUs for the insert are shown in Table 3-4. The HUs of 0-300 resulted in similar transmission values (i.e. agreement with ≤0.8% for both 6 and 23 MV). 200 HU (1.2434 g/cm^3) was chosen based on CT image data. Similarly in Table 3-5, board base HU combinations included were-300/-900, -200/-900, -100/900, -100/-850 and -100/-800 respectively for 'base shell' and 'base inside'. Results show that assigning -100 and -900 HU provided the best agreement (<0.4%) for 6 MV. For 23 MV, values agreed within 0.3%. -100 HU corresponds to a mass density of 0.9239 g/cm^3 and -900 HU to 0.1255 g/cm^3.

Typically, in order to incorporate external structures into treatment plans, there are two approaches. The first is to have the structure present during the CT simulation of the patient and the second is to have a contoured model in the TPS (21). The first will use attenuation information obtained from the CT while the contoured model will have a uniform HU assigned to the entire structure. Both approaches have their own advantages and limitations. While the first approach is the simplest, the accuracy of attenuation information can be affected by CT artifacts and the resolution of the image. Also, the larger field of view may also affect the accuracy of the CT HUs obtained (21). Since treatment couch tops are

different from the CT simulation couch top, it cannot be included in the planning CT image set and will have to be added during treatment planning. The second approach can allow more accurate representation of external structures but is more time consuming initially when manually contouring structures and matching attenuation information if it is not a default model which is available in the TPS. Contoured structures are also limited by the resolution that the TPS will allow. It is also important to have measured data for a wide range of gantry angles depending on what type of treatment is done on the external device and how probable the beam will be traversing through these structures. Since each model only has to be contoured once and after attenuation properties are matched between measured data and TPS calculated values, this model can be inserted into any plan easily and quickly and aligned accordingly to the patient.

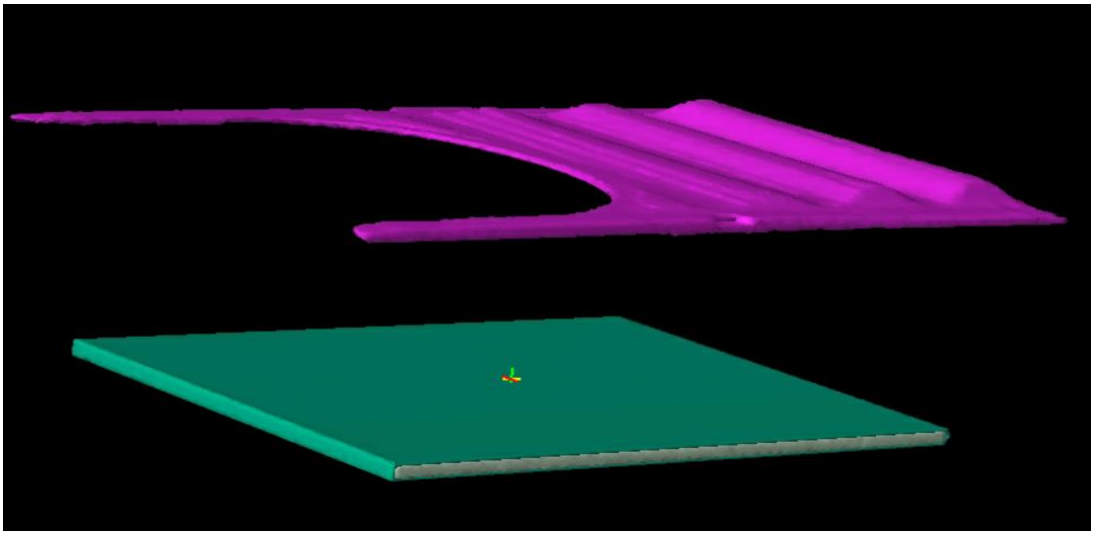

Figure 3-3: Custom Support Model of the ClearVue Prone Breast Board in the TPS. Top insert shown in magenta color and the board base, consisting of 'Base Shell' and 'Base Inside', shown in green and pastel yellow respectively.

Table 3-4: Top insert transmission factors of the treatment planning system custom model for various Hounsfield units for 6 and 23 MV

Gantry Angle	HU	(6 MV) 180	200	220	(23 MV) 180	200	220
Measured		0.983	0.973	0.976	0.999	0.993	0.990
	300	0.975	0.976	0.975	0.992	0.989	0.986
% Difference		0.8	0.3	0.1	0.7	0.4	0.4
	250	0.975	0.978	0.976	0.992	0.989	0.987
% Difference		0.8	0.5	0.0	0.7	0.4	0.3
	200	0.976	0.978	0.976	0.993	0.989	0.987
% Difference		0.7	0.5	0.0	0.6	0.4	0.3
	150	0.976	0.978	0.977	0.993	0.990	0.987
% Difference		0.7	0.5	0.1	0.6	0.3	0.3
	100	0.976	0.979	0.978	0.993	0.990	0.988
% Difference		0.7	0.6	0.2	0.6	0.3	0.2
	50	0.977	0.98	0.978	0.993	0.991	0.988
% Difference		0.6	0.7	0.2	0.6	0.2	0.2
	0	0.977	0.981	0.979	0.993	0.992	0.989
% Difference		0.6	0.8	0.3	0.6	0.1	0.1

Table 3-5: Board base transmission factors of the treatment planning system model for various combinations of Hounsfield units for 6 and 23 MV

		(6 MV)			(23 MV)		
	HU						
Gantry Angle		**180**	**200**	**220**	**180**	**200**	**220**
Measured		0.985	0.984	0.979	0.998	0.996	0.989
Base Shell	-300	0.986	0.988	0.986	0.996	0.996	0.992
Base Inside	-900						
% Difference		0.1	0.4	0.7	0.2	0.0	0.3
Base Shell	-200	0.985	0.987	0.984	0.996	0.995	0.992
Base Inside	-900						
% Difference		0.0	0.3	0.5	0.2	0.1	0.3
Base Shell	-100	0.984	0.987	0.983	0.995	0.995	0.991
Base Inside	-900						
% Difference		0.1	0.3	0.4	0.3	0.1	0.2
Base Shell	-100	0.982	0.984	0.981	0.995	0.994	0.990
Base Inside	-850						
% Difference		0.3	0.0	0.2	0.3	0.2	0.1
Base Shell	-100	0.981	0.982	0.979	0.994	0.993	0.989
Base Inside	-800						
% Difference		0.4	0.2	0.0	0.4	0.3	0.0

3.3.3 Clinically Acceptable Plan Incorporating Immobilization and Couch Structures

Figure 3-4A shows the dose distribution on a CT slice within the CTV (light blue) for Patient 4 "Plan 2" (Table 3-2 and 3-3, plan with breast board and Exact Couch rails "out"). The dark blue line outlines the tissue receiving 95% of the prescription dose. The 95% isodose line does not cover the CTV or the treated breast, which is not ideal. This demonstrates how the dose coverage was compromised due to external attenuating structures which are not taken into consideration. Figure 3-4B shows the dose distribution for a new plan that was created to take into consideration the immobilization and couch structures. The 95% isodose line in this case covers both the CTV and treated breast tissue well. For the new plan generated, the CTV V95 was 100% with a global maximum of 106.5% and the WB V_{95} was 94.4. Table 3-6 compares both the CTV V_{95} and WB V_{95} of the new plan, "Plan 2" and the originally intended plan coverage. A dose volume histogram (DVH) comparison (Figure 3-5) shows very similar curves between the new plan and the original clinical plan and a shifted curve to the left showing reduce coverage due to board and couch structures. DVH curves for the new plan of the contralateral and ipsilateral lung and heart are also similar to the original plan.

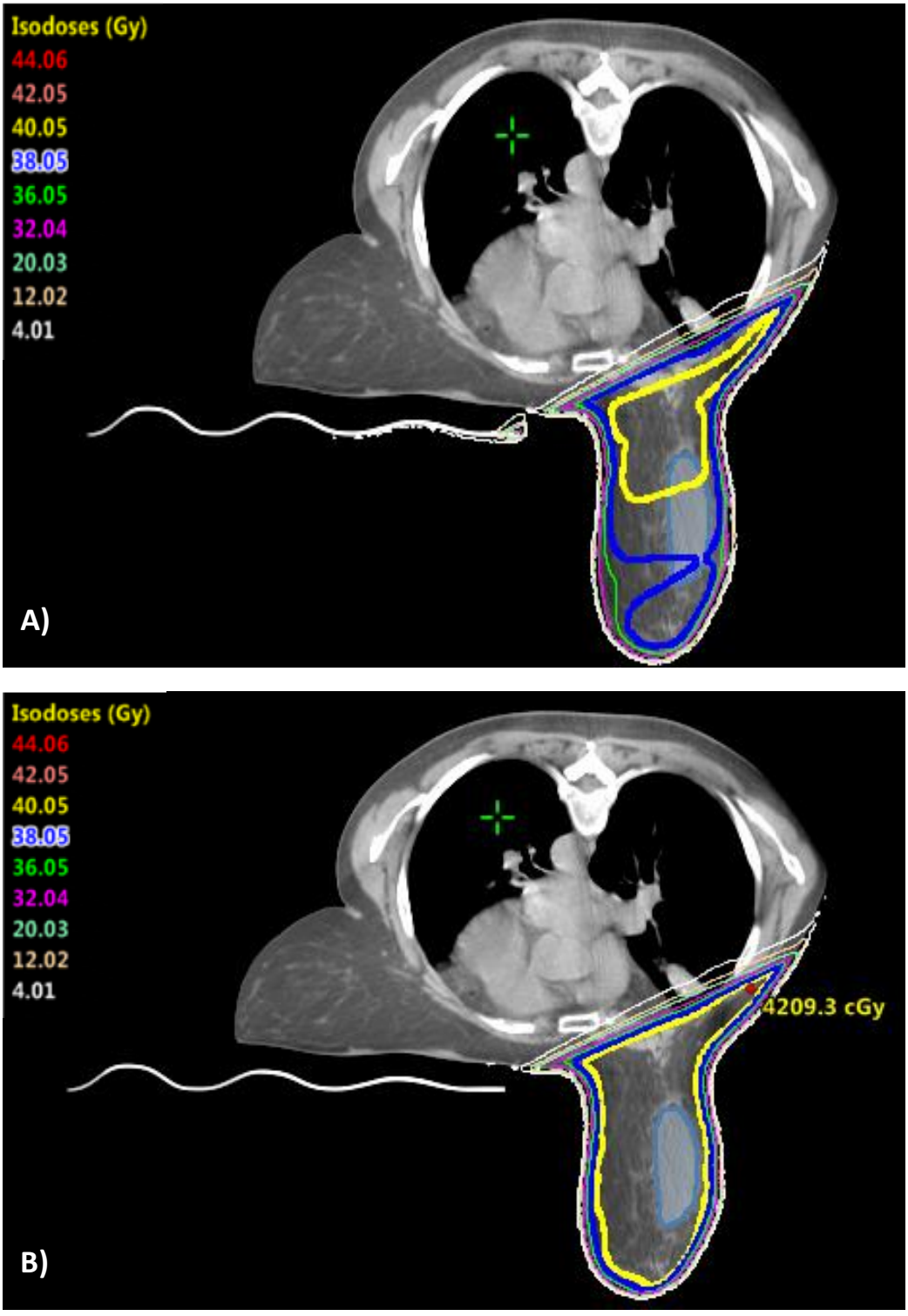

Figure 3-4: Dose Distribution Comparison of Compromised Target Coverage and New ECOMP Plan . A) Dose distribution calculated for "Plan 2" (Patient 4) with the breast board and Exact Couch with rails "out", B) Dose distribution of a new plan generated. CTV is outlined in light blue in A and B. 95% isodose line is in dark blue.

Table 3-6: CTV V95 and WB V95 comparison of new ECOMP plan with Plan 2 and originally intended plan.

	New ECOMP Plan	Plan 2 (Breast Board and Exact Couch rails "out")	Original Intent
CTV V_{95}	100.0	93.4	100.0
WB V_{95}	94.4	72.7	90.3

Figure 3-5: Dose volume histograms for the CTV and WB. Original clinical plan is shown with circles, Plan2 with squares and the new plan is shown with triangles.

Challenges faced during the treatment planning process to correct for the attenuation effect due to external structures included maintaining good WB coverage while keeping the maximum dose to what is clinically preferred by "painting down" hotspots. Different solutions to this include choosing a lower isodose line to prescribe to and adjusting the TPD which is chosen for electronic compensation. Emmens *et al.* (22) conducted a study correlating the compensation surface with breast size and the dose distribution in supine cases. They found that reducing the TPD, dose would be shifted resulting in reducing hot spots in the medial and lateral regions but increasing hotspots in the front of the breast, which was advantageous for patients with larger breast sizes. As TPD decreased, there was a decrease in the PTV_{95} and PTV_{107}. They also noted that there is a trade-off between minimizing maximum dose and maintaining PTV coverage. For larger separations, they would use a decreased TPD compared to smaller breast separations.

3.4 Summary

From the results in this chapter, reduced target as well as WB coverage is seen. The most compromise was seen with the Exact Couch which consisted of the highly attenuating rails. While the Exact Couch with rails "in" and Exact IGRT Couch had minimal effect on CTV coverage on most patients, a reduced WB coverage was still seen. This emphasizes the need to model external structures such as the couch top and immobilization board during the treatment planning process for accurate dose computation. This ensures sufficient dose delivery to the treated tissue and maintaining local control. A creation of a custom prone breast board model is demonstrated and outlined as well in this chapter for feasible clinical implementation. Only the attenuation effect was addressed in this chapter due to inaccuracies of the TPS algorithm when modelling dose deposition in the buildup region, the scatter and bolus effects will be discussed in the next chapter.

Chapter 4: Monte Carlo Study

4.1 Introduction

The "Monte Carlo method" was created In 1947. The first experiment which was similar to the Monte Carlo (MC) method was conducted by Comte de Buffon in 1777. The experiment involved repeatedly tossing a needle onto a ruled sheet of paper to determine the probability of the needle crossing with a line. In 1886, the mathematician LaPlace, proposed that the method of Buffon's experiment could be used to determine the value of π. The idea of the MC method was also involved in the development of thermonuclear weapons. In 1949, the first founding paper "The Monte Carlo Method" was published on the Monte Carlo methods and here, "Monte Carlo" was associated with stochastic sampling. An area that greatly utilizes MC methods is for research in medicine, which contributes to approximately 10 % of published work on MC (23).

A general definition of the MC method is that it is a stochastic method that is used to solve equations or calculate integrals using random number sampling (23). The basic math theorem of the MC method is the Central Limit Theorem. Based on this theorem, the distribution of what is sampled will follow a normal distribution with a mean and standard deviation. If the sample size is very large, the sample mean will be the same as the population mean, (i.e. the true value). In the context of medical physics, MC has applications in radiation dosimetry, patient dose calculation and more. MC techniques simulate random trajectories of particles by using random numbers to sample from probability distributions of the physical processes that can take place (24). Physical processes which take place are dependent on the atomic interaction cross sections which can change with the energy of the particle and atomic number of the material it is in (24).

Photons can commonly undergo Compton (incoherent) scattering around 1 mega-electron-volts (MeV) where the photon scatters and sets an electron in motion, resulting in a "hole", which will later have to

be filled by another process. When photons enter the higher MeV range, the dominating process will be pair production (threshold = 1.022 MeV). This is where the photon interacts with the electromagnetic field of the nucleus, is absorbed and an electron-positron pair is created. Triplet production (threshold = 2.044 MeV) can also happen if the interaction is between an electron and the photon and energy is also imparted to the electron and is freed. At lower energies, the dominant process is the photoelectric effect where the photon is absorbed and an electron freed from the inner shells. Another physical process is Rayleigh (coherent) scattering where the photon scatters elastically from structures in the material and no energy is lost. The dominating process in a 6 MV beam is Compton scattering for soft tissues as well as the immobilization board and couch studied in this work. Figures 4-1 illustrates the energy ranges and atomic numbers where each interaction type is dominant (35). Figure 4-2 illustrates the main photon interactions in matter (36).

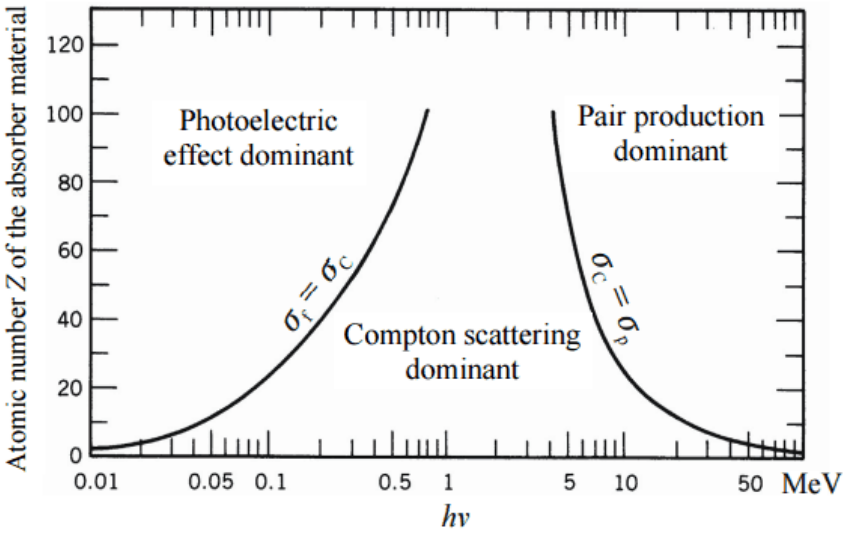

Figure 4-1: Dominating photons-matter interaction types depending on energy and atomic number; Adapted from "Interaction of Gamma Radiation with Matter". https://www.nuclear-power.net/nuclear-power/reactor-physics/interaction-radiation-matter/interaction%20-gamma-radiation-matter/

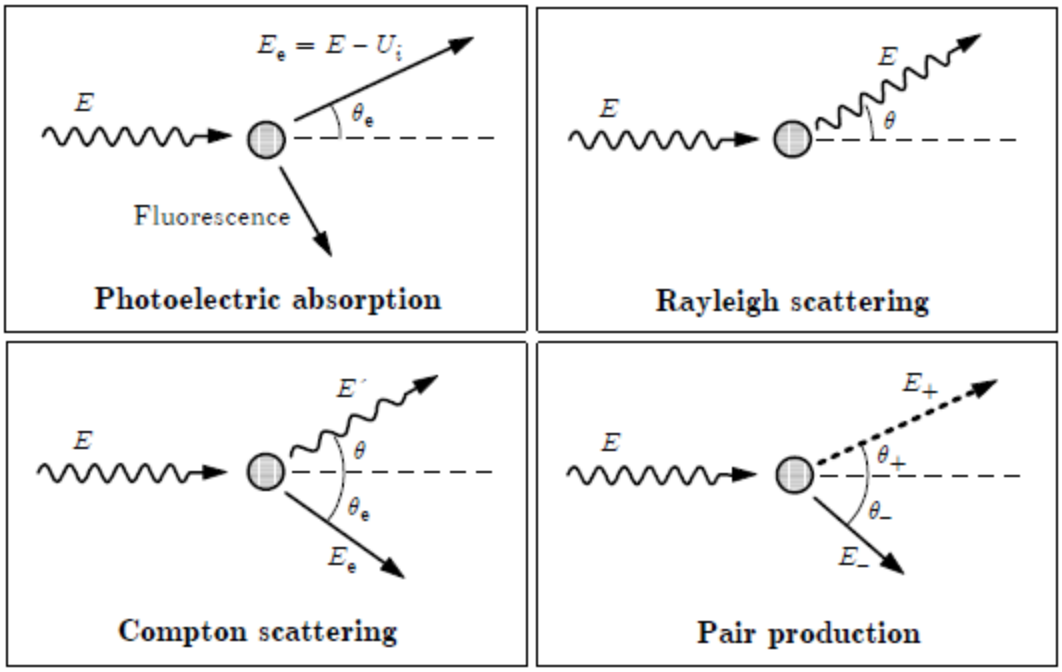

Figure 4-2: Illustration of main photon interactions in matter. Adapted from "PENELOPE-2014: A Code System for Monte Carlo Simulation of Electron and Photon Transport" https://www.oecd-nea.org/science/docs/2015/nsc-doc2015-3.pdf

Electrons and positrons lose energy as they travel through matter by inelastic collisions with bound electrons. These particles can also both lose energy in the vicinity of a nucleus and as a result a photon would be produced. Annihilation can also take place between an electron and positron producing a pair of 511 keV photons.

In order to employ the MC method to radiation transport simulations, several components are required. These are: random number generation processes, methods for sampling from a probability density function, the energy dependent atomic cross section information used to generate these functions, a routine for "scoring" of dose results, geometrical models and physical material information. A large sequence of random numbers is needed to solve a complex problem. In this situation it is important that the sequence itself is sufficiently large and numbers within the sequence do not depend on each other so that results of a MC simulation are not correlated (25).

Several studies in literature have compared the accuracy of MC methods to existing TPS dose calculation algorithms especially in the buildup region and the interface of sharp density changes. Panettieri *et al.* (27) conducted a study comparing the accuracy of the Analytical Anisotropic Algorithm (AAA) and Pencil Beam Convolution (PBC) dose calculation algorithms in the Eclipse TPS with the MC calculations. Their results showed that both AAA and PBC underestimate the dose especially within the first 2 mm of the surface for a selected oblique gantry angles. They also noted that some chambers would overestimate doses near the surface due to their design. Guebert *et al.*(28) looked at a comparison between AAA and Acuros External Beam (AXB) through a in the context of clinical implementation for breast plans. AXB in literature has shown to have the best agreement with MC results (within 5%). Their results showed large differences between both in the mean superficial dose by a median of 3.2 Gy. Their superficial region was defined as a 5 mm margin deep into the body contour. They also reiterated from another study that AAA tends to agree with MC better than older calculation algorithms but is not very accurate in superficial dosimetry. The threshold for skin reactions, such as transient erythema, is 2 Gy (29). Having more information about superficial doses that may not be available in the TPS can prove to be helpful for clinicians for breast treatments. This chapter details research that utilized the MC method for patient dose calculations in order to provide more accurate dosimetric information pertaining to the buildup region.

4.2 Material and Methods

4.2.1 EGSnrc

Electron Gamma Shower – National Research Council (EGSnrc) is a software package that is used for MC simulations which includes photon and electron transport in any geometry for particles that range from a few kilo electron volts to a few hundred giga electron volts (30). It is a version of the EGS4 system with

additional modifications. EGS originates from code developed in the early 1960s by H.H Nagel. EGSnrc takes into account a broad range of physical process in its simulations. EGSnrc uses information provided by PEGS4 which include material cross section and branching ratio data (30). DOSXYZnrc is an EGSnrc-based code that was used for dose calculations in a phantom and energy deposition can be scored within the voxels of the phantom. Information that are relevant to the simulation (phantom, treatment parameters, source types, number of histories, etc.) are all put into an input file, shown in Figure 4-3. Materials that are used in MC simulation are in a data file that is available within EGSnrc. DOSXYZnrc allows many source types with different geometries. There is also graphical use interface that can create input files. The BEAMnrc code is what allows users to model linear accelerators (linac) and its individual component with the appropriate properties. The linac that was used in this study was a pre-existing model of the Varian Trilogy at our institution that was built and used in previous works. DOSXYZ_show is another feature that was used to visualize the phantom and dose distribution across its slices. It allows a user to view in different planes (i.e. x-y, x-z, y-z planes). Coordinate, density and point dose information is also available. The coordinate system used in EGSnrc can be described as positive x to patient right, positive y to patient feet and positive z to patient posterior for a head first prone position. Two other types of files that were frequently used were egsphant and 3ddose files. An egsphant file contains information for the simulation and also for DOSXYZ_show to display density information. It can be based on CT image data or manually coded. Creation of an egsphant file will be described in section 4.2.2. The information that is located in an egsphant file includes the number and names of media in the phantom used, number of voxels in each direction, voxel boundaries in each direction and the media number and density information for X-Y arrays for each z-slice. Dose information is output in a 3ddose file format in arrays along with voxel number and boundary information.

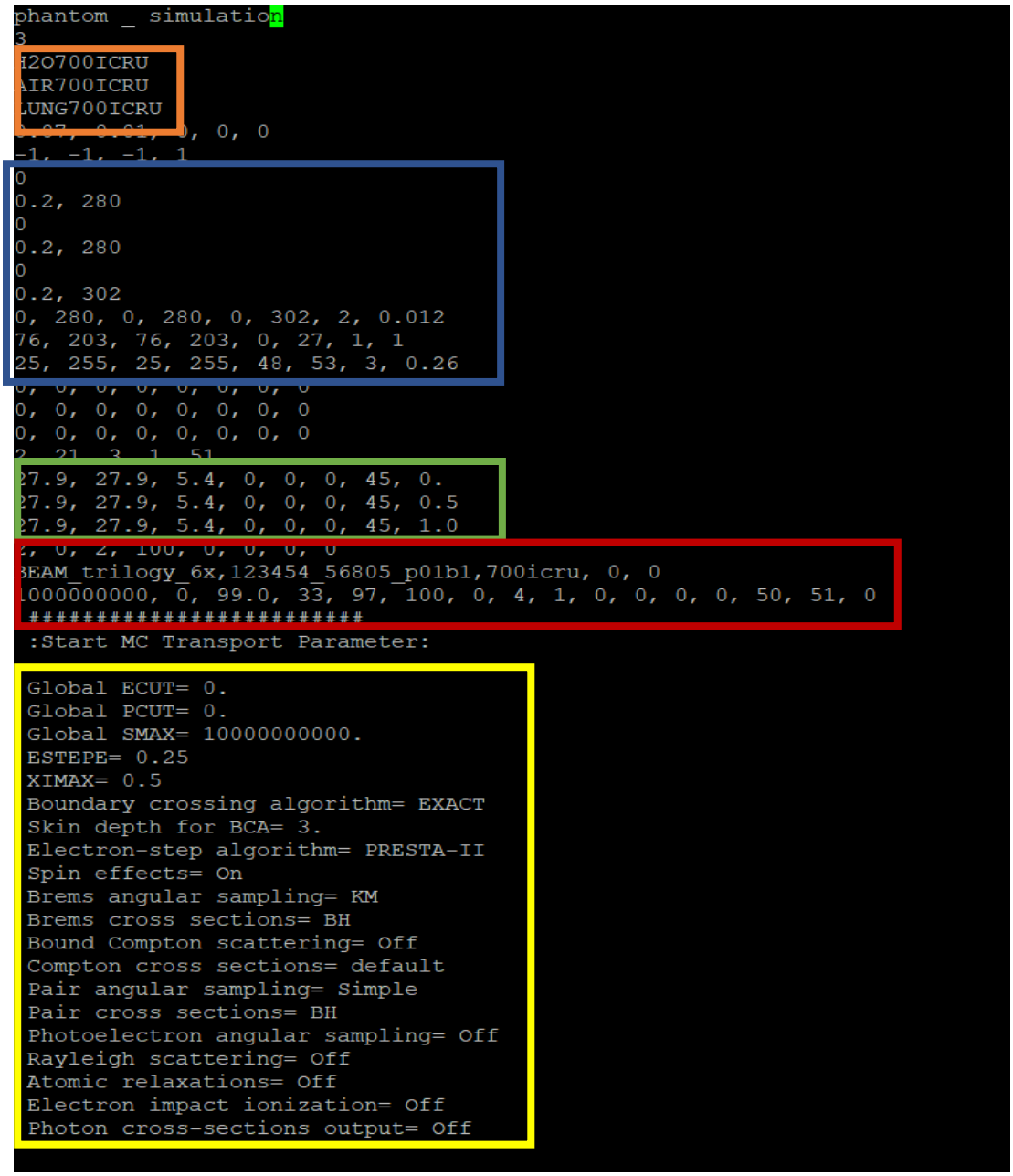

Figure 4-3: Example of a input file used in DOSXYZnrc . Material information (orange), phantom information (blue), treatment parameters (i.e. isocenter, gantry angle)(green), linear accelerator model and history information (red) and MC settings (yellow)

4.2.2 McGill Monte Carlo Treatment Planning System, CERR and Other Software Tools

The McGill Monte Carlo Treatment Planning system (MMCTP) is a program where patient treatment planning can be combined with MC dose calculations (31). It has many features including visualization

options for CT images, treatment planning tools (i.e. treatment beam options, contouring) and MC file generation for BEAMnrc and DOSXYZnrc and dose analysis. For the purposes of this work, MMCTP was only used for egsphant file generation from CT image sets. Prior to creating the phantom file, appropriate files must be exported from the clinical TPS. This includes the CT image set, structure set, plan dose and treatment plan file.

During the process of generating an egsphant file, there are four tabs or options. Firstly, the "Contour Settings" allow use and assignment of a material and density to any contour chosen. Also, the user can choose to assign a density to the surroundings of a specific contour through the "Clean External Contour" option. In the "CT settings", the user can choose a CT number to density conversion curve (CT ramp) that converts Hounsfield unites (HUs) to a physical density and also choosing a material type. The CT ramp that was used for patient simulations is shown in Figure 4-4. For phantom studies, adjustments were made using appropriate HUs, material type and the corresponding densities.

Material	HU Low	HU High	Density Low (...	Density High (...
AIR700ICRU	-1050.	-985.	0.001	0.001
LUNG700ICRU	-985.	-810.	0.001	0.24
ICRUTISSUE700I...	-810.	85.	0.24	1.19
ICRPBONE700I...	85.	4000.	1.19	3.75

Figure 4-4: CT number to density conversion curve used in patient simulations. -1050 HU $\leq$ air $\leq$ -985 HU; -985 HU $\leq$ lung tissue $\leq$ -810 HU; -810 HU $\leq$ tissue $\leq$ 85 HU and 85 HU $\leq$ Bone $\leq$ 4000 HU

Similar to the "Contour Settings" option, the user can manually assign a material and density to specific voxels in the "Manual Settings" option. In the final tab, the user can input the egsphant limits and voxel resolution. The limits dictate the size of the phantom used in the simulation and they can be determined by measuring the distance from the user origin in the TPS for the x, y and z direction and then applying

the DICOM offset. The DICOM offset is the translational transformation applied to the CT image set center to result in the user origin. This is a user specified point that serves as the origin (0,0,0) of the reference frame used in a treatment plan. Generally, it is preferred to have the egsphant limits match the dose calculation grid that was used in the TPS treatment plan for comparison of the two. Egsphant limits also have to be increased to include regions of the couch top to encompass the whole breast board and to incorporate any external structures into the phantom.

Computation Environment for Radiological Research (CERR) is a software platform that is written in MATLAB. There are various tools in CERR that allow analysis and comparisons of dose and images. It allows users to import and display treatment plans from different treatment planning systems. This software was used to convert the 3ddose files that were obtained from a MC simulation and combine them into one for comparison to a calculated dose distribution from the TPS.

MC simulations were run using the Center for Computation Research (CCR), an academic supercomputing facility, which allowed for dose calculations by employing parallelization. The SSH client PuTTY was used to interface with and submit jobs to the CCR, where a local copy of EGSnrc was used to run and edit code. Finally, the freely available File Transfer Protocol (FTP) program, Filezilla was used to transfer files back and forth between local storage to the CCR where it could be used (e.g. phantom files, dose files, etc.)

4.2.3. MC Simulations

4.2.3.1 MC Validation and Calibration Factor

Although our existing virtual model of the Trilogy linac with 6 MV energy has been validated in previous works at our institution, there was a need to carry out independent validation in the context of this

study. A water phantom was coded into the input file directly with dimensions of 50x50x40 cm^3 with a 10x10 cm^2 field size and a source to surface distance (SSD) of 100 cm. 10^{10} particles were used for the simulations with voxel dimensions of 0.2 cm. Percent depth dose (PDD) curves were obtained by recording point doses along the central axis (CAX) using the EGSnrc tool DOSXYZ_show. Profiles were obtained perpendicular to the CAX in both directions in a similar matter at depths of 1.5 cm and 10 cm. These curves were compared to TPS data with similar geometry.

A calibration factor was obtained following the method described in the study conducted by Bhagroo *et al.* (32) to correlate the dose that is obtained in a MC simulation which is given in units of Gy/particle to an absolute dose unit of Gy, which is reported by the TPS. This is done by mimicking the setup in the simulation in the TPS (100 monitor units (MUs), 100 SSD, 10x10 cm^2 field size). A ratio is then taken between the doses at the depth of the maximum dose (d_{max}) on the CAX. The units of the calibration factor is given by:

$$F_{cal} = \frac{dmax\ in\ TPS\ [\frac{Gy}{MU}]}{dmax\ in\ MC\ [\frac{Gy}{particle}]} = \frac{particle}{MU} \quad (4)$$

4.2.3.2 Phantom Simulations

There are two approaches to incorporating the phantom density and material information into input file. The first approach, code-based, is to manually code material and density information into the input file directly (i.e. blue section in Figure 4-3). An egsphant file of the coded phantom will be output at the end of the simulation to be used in DOSXYZ_show. The second approach is to use density information obtained through the CT image set itself, CT-based, and use a CT ramp or manual assignment for material and density information (done in MMCTP). This information is then included in the egsphant file created that is referenced in the input file and used in the simulation. Both were used in the MC verification of shallow depth measurements results which were acquired in Chapter 2, section 2.2.3. A

similar setup as that in Figure 2-5C was modelled in an input file shown in Figure 4-5. From experimental results, the effect of different gantry angles had a minimal effect on values, therefore simulations were only done at 180 degrees. The phantom was assigned to be the material and density of water and a custom density correction file (independent of the default density correction files for different materials included in EGSnrc) was created to represent the material and density of the board base. The board base was represented as a uniform thickness. To better represent the structure of the board base, simulations were also run with a sandwich structure described in

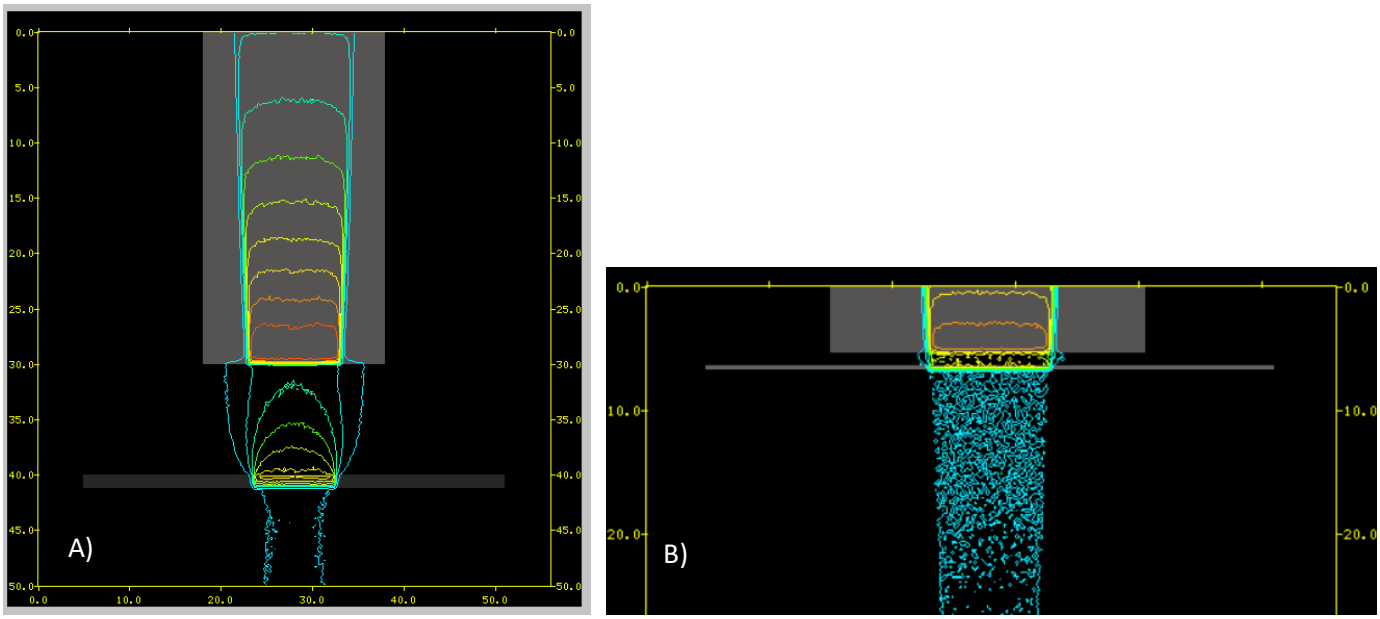

Figure 4-5: Phantom simulations shown through DOSXYZ_show. A) Scatter effect simulation setup, B) Bolus effect simulation setup. Direction of gantry angle is 180 degrees.

Chapter 3. Similarly, custom density corrections were created to best represent the density used in the TPS custom model. Point doses were taken at the surface, 0.3 cm and 0.5 cm along the CAX and compared to measured and TPS results. Uniform densities looked at for the breast board were 0.3 and 0.2 g/cm^3 based on CT image HU information.

Density correction files are created using data from the ESTAR web application that is provided by the National Institute of Standards and Technology (NIST). ESTAR allows materials that are not included in

EGSnrc to be used in MC simulations. A density correction file has a 3-line header that has to be included when put into EGSnrc. This includes a description of material, number of energies, mean ionization energy, density, number of elements, atomic number and the mass fractions of each element. The data portion that follows is copied directly from ESTAR which is the density effect parameter for a list of selected energies that must be used. The density effect parameter or density-effect correction that is calculated takes into consideration the reduction of the stopping power of the material due to polarization by an incident electron. This density correction file can then be transferred to the correct EGSnrc directory for use in a simulation. When custom density correction files are used in a simulation, adjustments have to be made to the input file. In particular, there will be a media definition section included where the nominal density of the material(s) as well photon and electron cutoff values are listed.

To verify the measured bolus effect results, a simplified geometric model was used. The insert was represented by a thin, 4 mm uniform thickness. The material chosen was polymethylmethacrylate (PMMA) which had a similar density to the insert of 1.19 g/cm^3. The simulation set up included a water phantom and the flat insert. An air gap was left to represent the foam cushion. Two air gaps (2.4 and 1 cm) were looked at to observe the change in the bolus ratio (equation 2) with a patient laying on the cushion. A simulation was done with and without the insert contour in order to calculate the bolus ratio.

A simple scatter analysis was carried out for the scatter and bolus simulations which followed the method used in a study by Grey *et al*. (33). The scatter component of dose with the board at a certain depth is calculated with the follow equation:

$$D_{scatter} = D_{with\ board,\ depth} - (D_{without\ board,depth} \times TF) \quad (5)$$

To use equation (5), doses in EGSnrc will need to be converted to absolute dose in cGy. This is done by using the following equation:

$$Absolute\ Dose\ (EGSnrc) = \ EGSnrc\ Dose\ \left[\frac{Gy}{Particle}\right] x\ F_{cal}\left[\frac{Particle}{MU}\right] x\ MU\ x\ \frac{100\ cGy}{Gy} \quad (6)$$

4.2.3.3 Simulation of Patient Case

To determine the clinical relevance of MC simulation results, a patient simulation was run. Figure 4-6 outlines the workflow to run a patient simulation. The relevant files were exported from the TPS and additional information such as the dose grid size and phantom limits were also obtained. The CT images and structure set file were imported into MMCTP. To minimize fluctuation and incorrect assignment based on varying HUs outside and inside the patient body with the CT ramp shown in Figure 4-4, the surroundings outside of the body were set to air. Only the effect of the insert was looked at for the patient case. The material assigned to the insert was PMMA (1.19 g/cm^3). An in-house input file generator was used to create the input required for the simulation. With information extracted from the plan file, the input file generator will write all multileaf collimator (MLC) position information from the treatment plan into the input file. All files were transferred to the CCR. Resulting dose files were downloaded, combined and analyzed in CERR and compared to an Eclipse calculated plan. A subtraction was taken to see the difference in buildup doses.

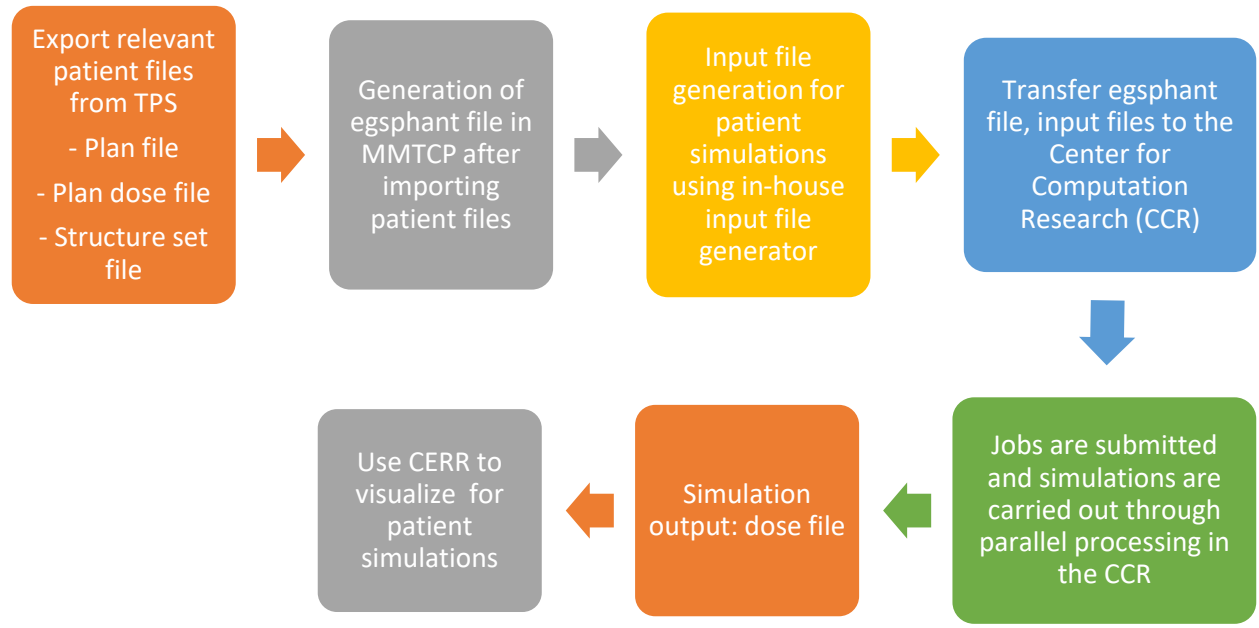

Figure 4-6: Patient simulation MC workflow

4.3 Results and Discussion

4.3.1 MC Validation and Calibration Factor Calculation

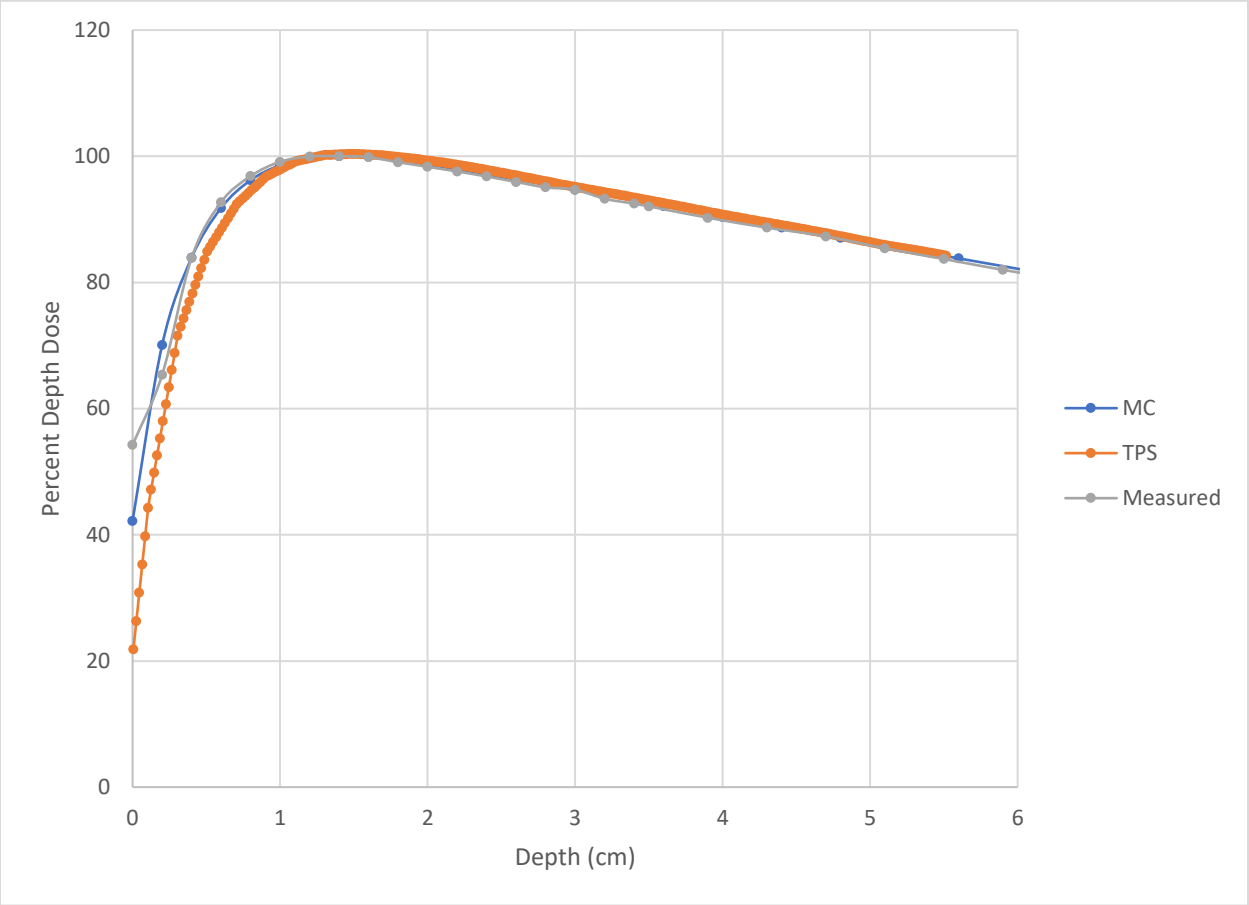

Figure 4-7: Percent Depth Dose curves for 6 MV with 10x10 cm^2 field size. MC calculated (blue), TPS calculated (orange) and measured (grey).

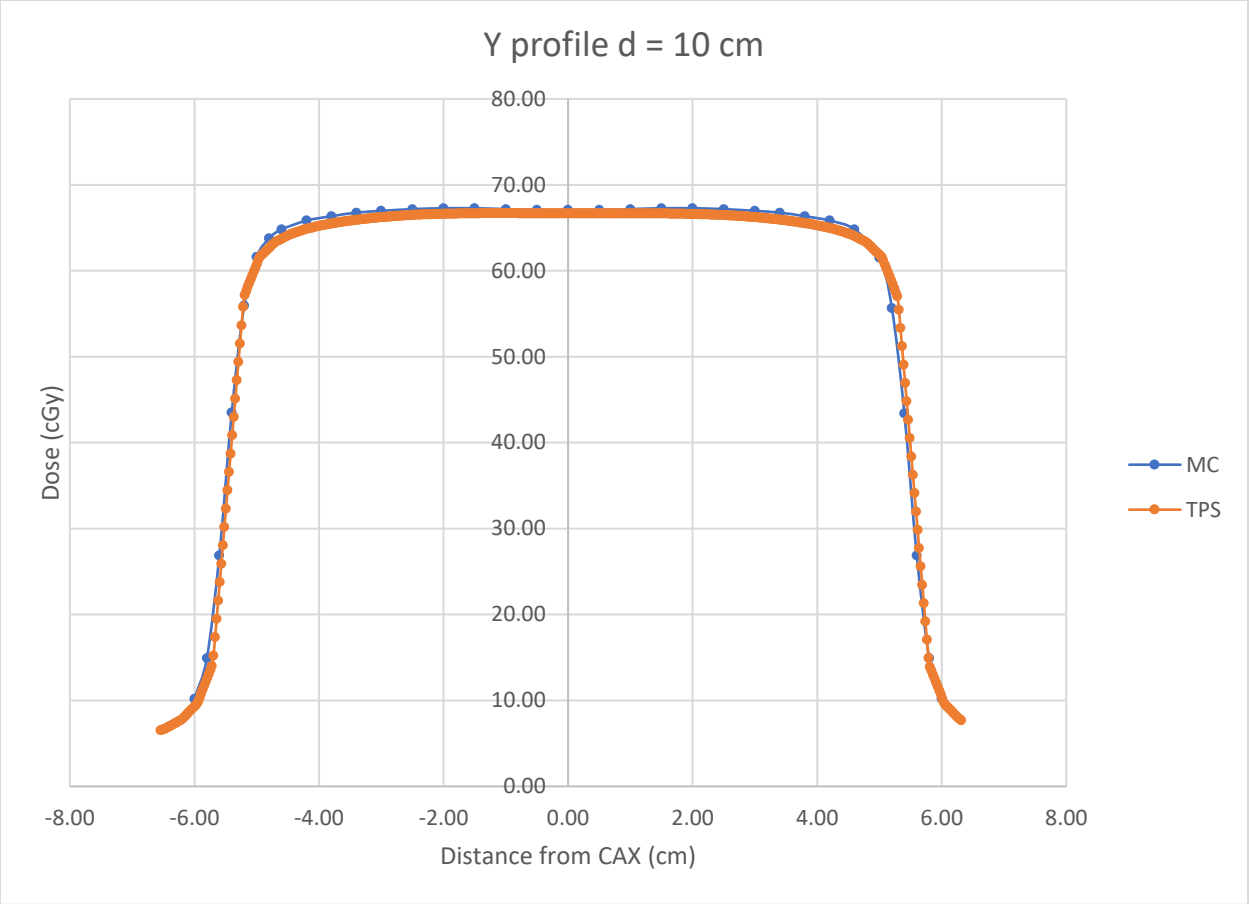

Figure 4-8: Profile at depth = 10 cm for a 10x10 cm^2 field size, 6 MV. MC calculated (blue) and TPS calculated (orange).

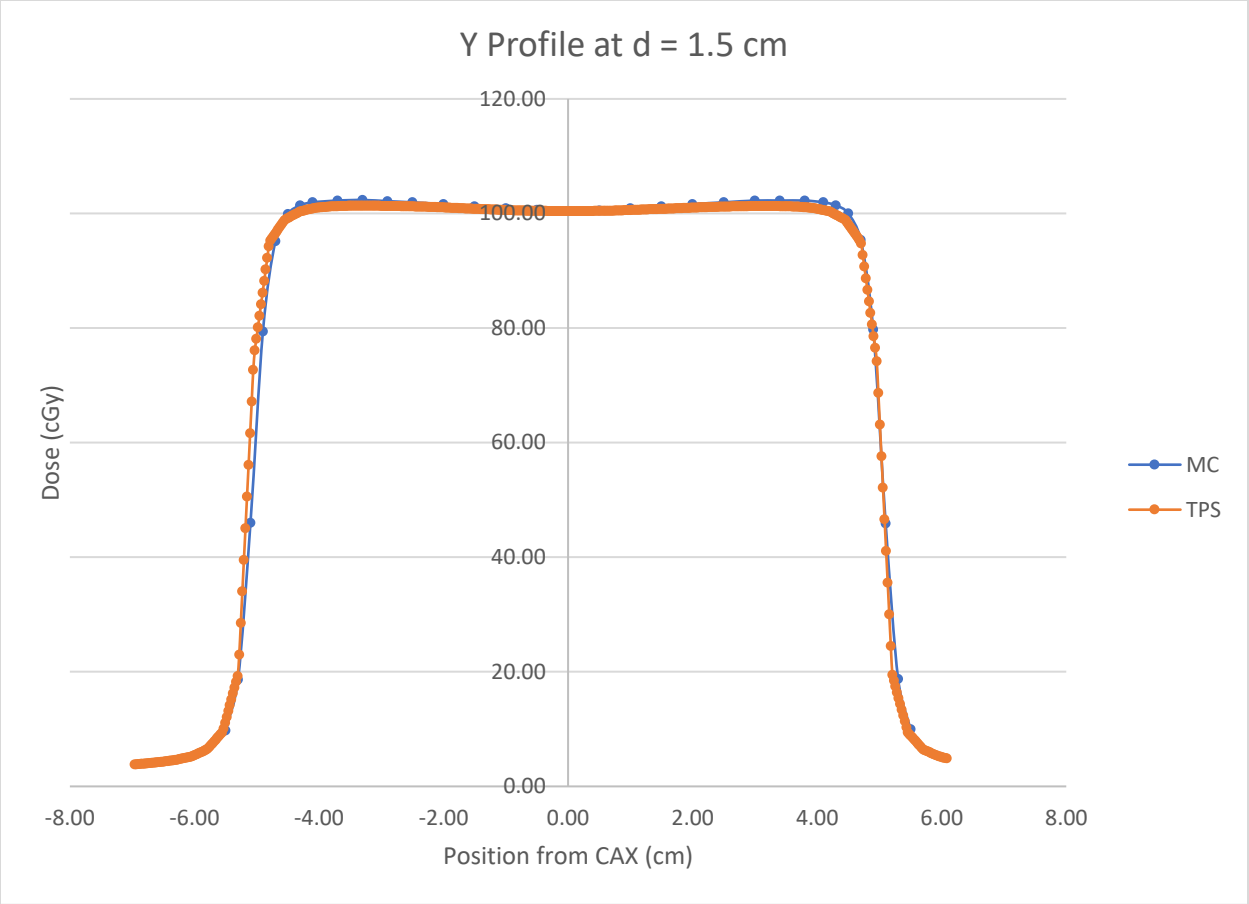

Figure 4-9: Profile at depth = 1.5 cm for a 10x10 cm^2 field size, 6 MV. MC calculated (blue) and TPS calculated (orange).

Calculation of Calibration Factor, F_{cal} is as follows:

Dose at depth of 1.5 cm (depth of maximum dose, d_{max}) in TPS = 0.01004 Gy/MU

Maximum dose obtained in MC in phantom (10^{10} particles) = 1.47x10^{-16} Gy/ particle

Dose % at dmax (d=1.5cm) in MC = 99.6%

$$F_{cal} = \frac{0.01004\ \text{Gy/MU}}{0.996\ x\ 1.47\text{x}10{-}16\ \text{Gy/ particle}} = 6.99\text{x}10^{13}\ \text{particle/MU}$$

Figure 4-7 to 4-9 show the PDDs and profiles obtained from MC and the TPS. All profiles that were obtained from MC simulations generally agree with the TPS profiles within 1.5%. There are some discrepancies seen in the PDDs between TPS and MC, which could be due to the inaccuracies of the TPS algorithm in the buildup region. Also, the volume averaging with depth as a result of using the voxel size of 0.2 cm could shift the MC curve slightly. However, MC and measured results for the PDD agree well except for at the surface point. All three curves agree well at depth of maximum (i.e. 1.5 cm) and beyond.

4.3.2. Phantom Simulations

Table 4-1: TPS results for scatter ratios of the board base

Air Gap			
	0 cm	**0.3 cm**	**0.5**
10	0.36	0.88	0.94
8	0.33	0.87	0.94
6	0.38	0.88	0.94
4	0.36	0.87	0.94
2	0.31	0.87	0.93
0	0.34	0.87	0.94

Table 4-1 shows scatter ratios (determined by equation 3) at the surface, 0.3 cm and 0.5cm of a phantom setup as a function of air gap with the board base. These values change relatively little, if at all, with changing air gap at any depth. This demonstrates that the AAA dose calculation algorithm might

not provide accurate dose information at shallow depths and therefore no useful information about skin dose.

Figure 4-10 shows MC generated scatter ratio curves along with the “no scatter” reference curve. With a decrease in air gap from 10 cm to 0 cm, it is shown that the scatter ratio increases from 0.65 to close to 0.9. With depth, this air gap effect is less and less pronounced. This trend is similar to the measured results in Figure 2-10. Figure 4-11 shows surface ratios normalized to the reference surface ratio, starting at 1.5 times the reference to over 2 times which was similar to Figure 2-11 results.

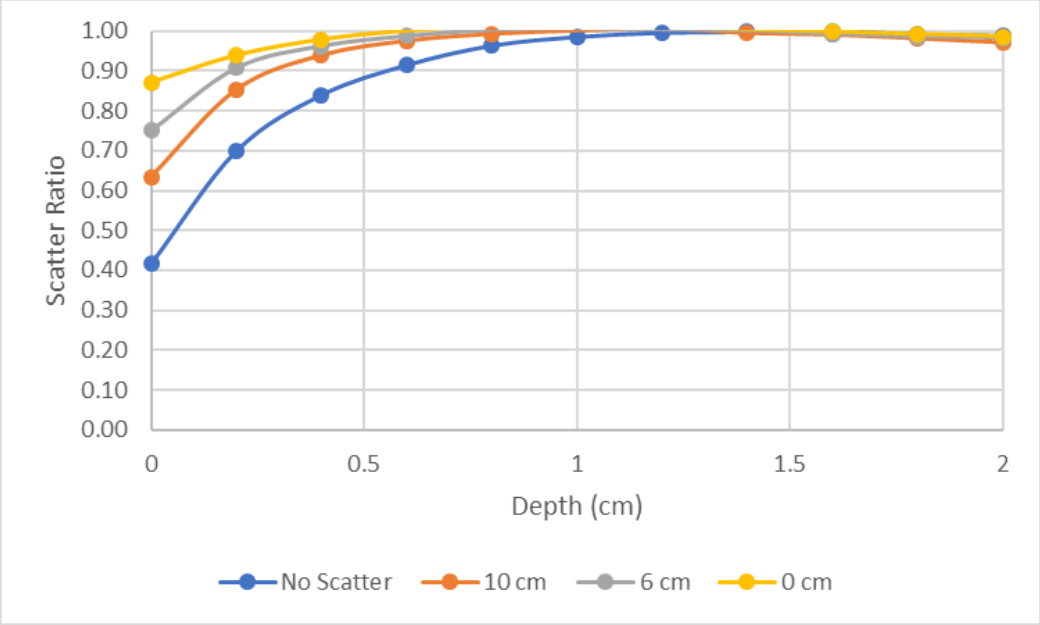

Figure 4-10: MC scatter ratios for selected air gaps of 10 cm (orange), 6 cm (grey) and 0 cm (yellow).

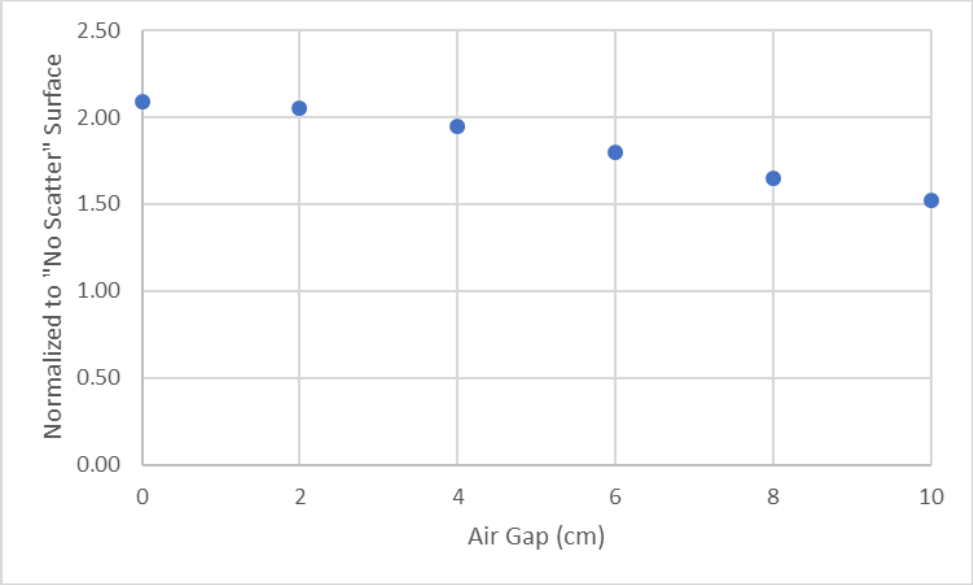

Figure 4-11: MC scatter ratios normalized to “no scatter” reference surface dose.

Figures 4-12 to 4-14 show MC scatter ratios at depths of 0cm, 0.3 cm and 0.5 cm compared to TPS and measured results. Trends are all similar to the measured curve except the TPS curve. Given that MC is considered the most robust of dose calculation methods, this provides evidence that the TPS calculated values deviate from experimental measured values. The air gap effect once again is most noticeable with 0 cm depth compared to greater depths where the trend is almost constant (e.g. depth of 0.5 cm). Large differences with measured results are seen especially at the surface of the phantom (>15%) with each density looked at. These differences decrease with increasing depth. This again could be due to limitations of performing surface dose measurements with an ion chamber. Of the three densities looked at, the “sandwich structure” agreed the most with measured results. Densities used for the simulation were obtained from the densities used in the TPS. The composition of the board base is not known and was estimated. This was also limited by the availability of material data that could be used for custom density files.

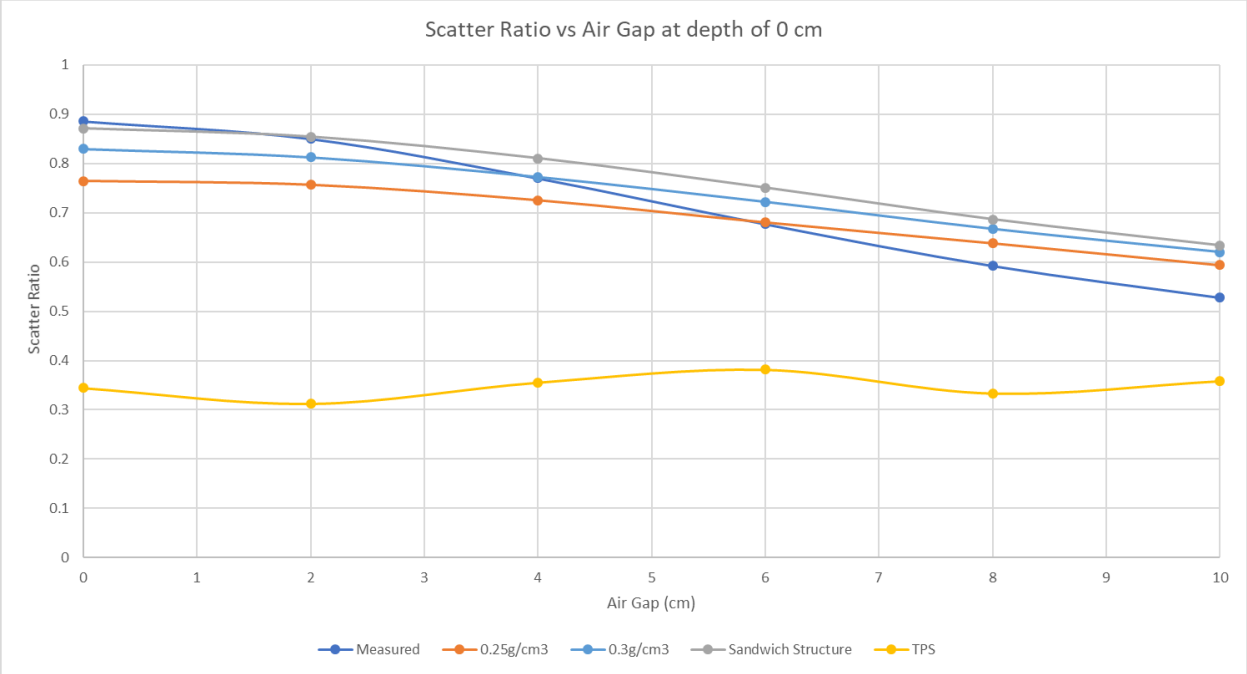

Figure 4-12: Scatter Ratio vs Air Gap at depth of 0 cm. Measured (blue) results, TPS (yellow) and different densities chosen for the board base are shown. 0.25 g/cm^3 (orange), 0.3 g/cm^3 (light blue) and sandwich structure (grey) densities are chosen.

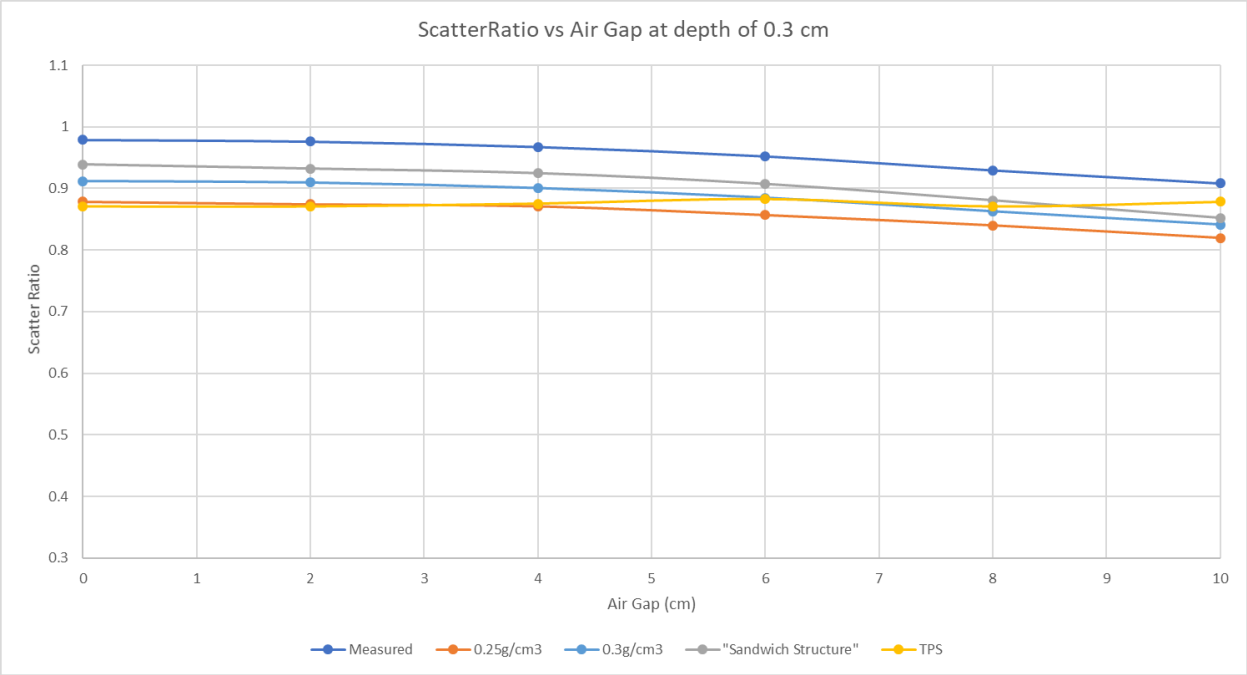

Figure 4-13: Scatter Ratio vs Air Gap at depth of 0.3 cm. Measured (blue) results, TPS (yellow) and different densities chosen for the board base are shown. 0.25 g/cm^3 (orange), 0.3 g/cm^3 (light blue) and sandwich structure (grey) densities are chosen.

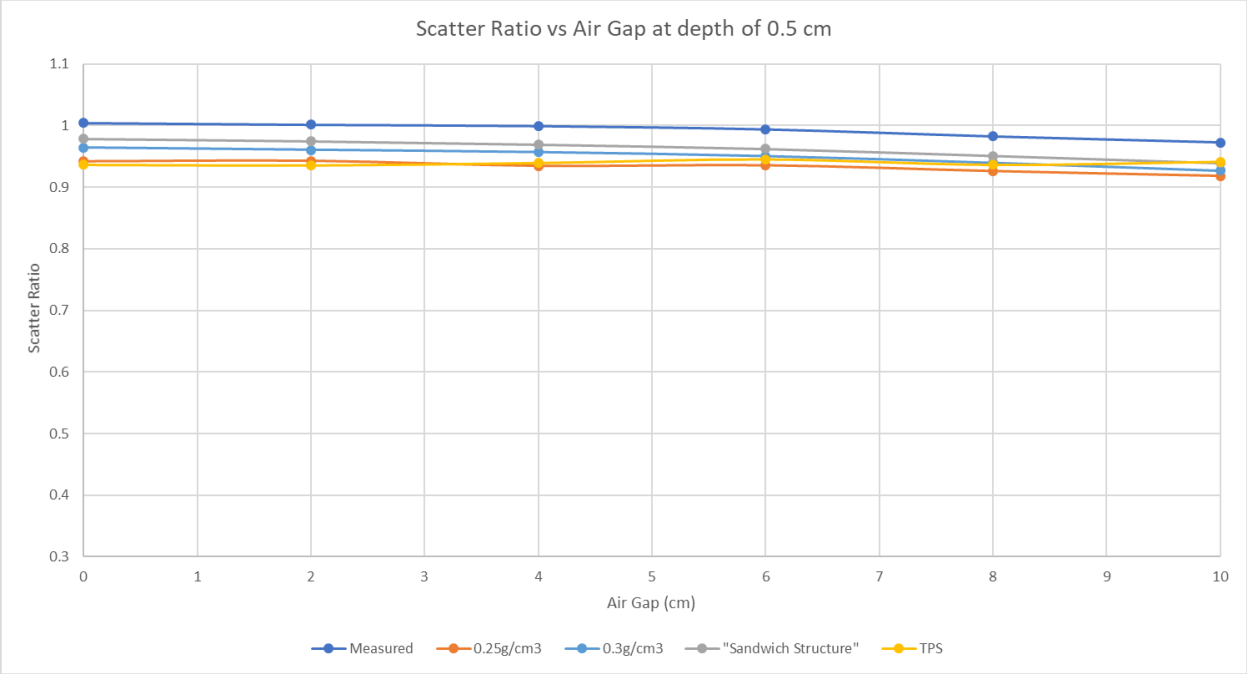

Figure 4-14: Scatter Ratio vs Air Gap at depth of 0.5 cm. Measured (blue) results, TPS (yellow) and different densities chosen for the board base are shown. 0.25 g/cm^3 (orange), 0.3 g/cm^3 (light blue) and sandwich structure (grey) densities are chosen.

Figure 4-15 shows the scatter components of doses recorded at a depth of 0 cm in MC simulations with the board modelled. The scatter component is the additional dose from the presence of the board base. Reference shallow depth doses without the board are 43 cGy, 73 cGy and 87 cGy at depths of 0 cm, 0.3 cm and 0.5 cm respectively and a d_{max} dose of 100 cGy. Overall, there is an increase to the scatter components of dose with decrease in air gap. At 10 cm air gap, values range from 17 cGy to 21 cGy across the three densities looked at for the board base. This number increases to a range of 34 cGy to 45 cGy for the air gap of 0 cm. Figure 4-16 shows the scatter components of doses recorded at depths of 0 cm, 0.3 cm and 0.5 cm in MC simulations with the "sandwich structure" version of the board base. Similar to the trend in the scatter ratio curves with depth in Figure 4-12 to 4-14, the scatter components to doses at depths are 0.3 cm and 0.5 cm are less affected by the change in air gap.

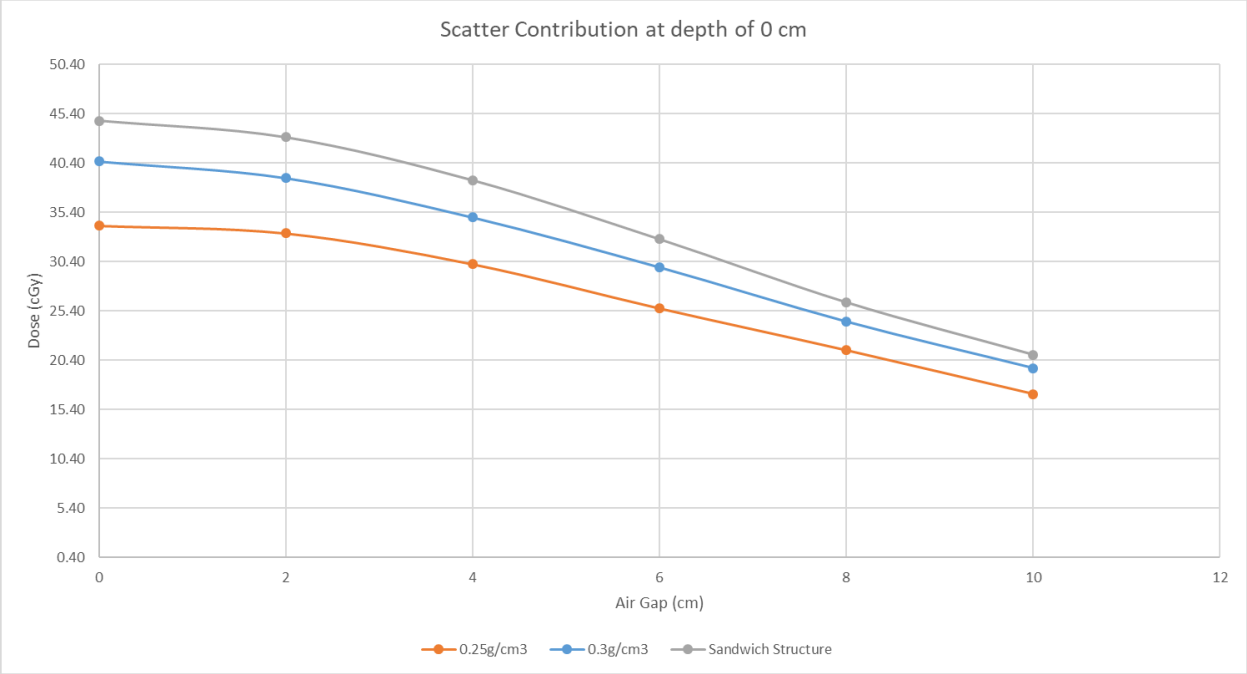

Figure 4-15: Scatter contribution to doses at the surface from the board base for different densities chosen.

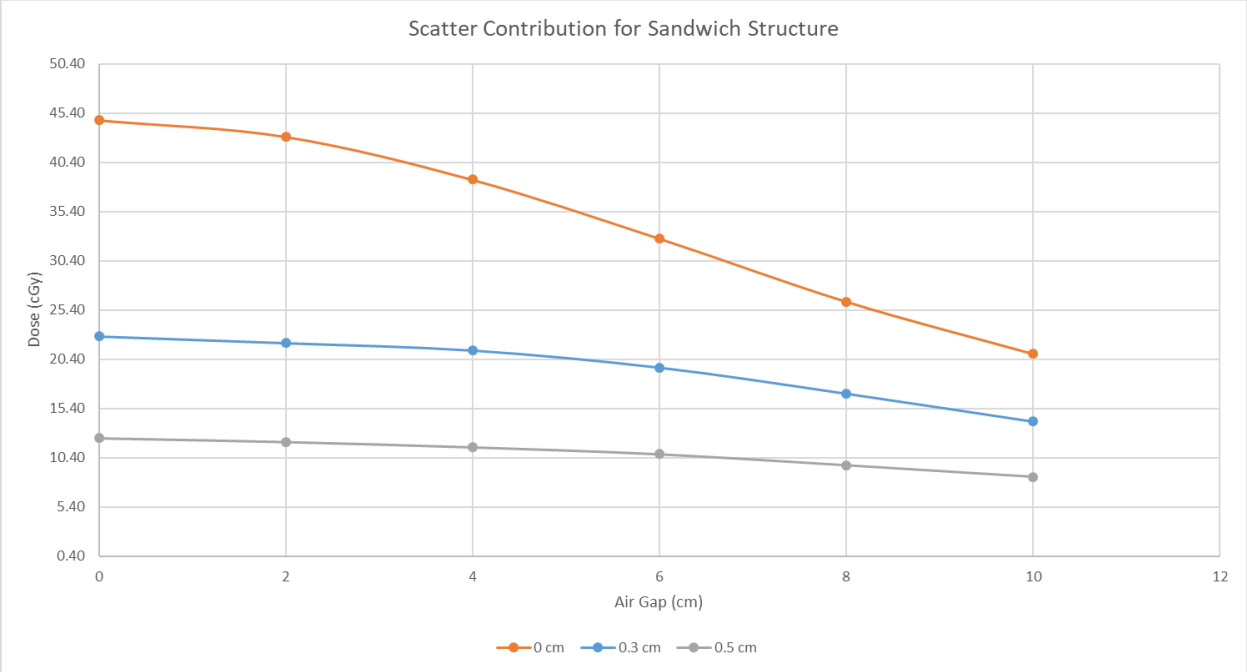

Figure 4-16: Scatter contribution from modelled board base for depths of 0cm, 0.3 cm and 0.5 cm for Sandwich Structure densities.

Table 4-2 Bolus Ratios for MC Simulations Modelling a Simplified Version of the Insert

	Gantry Angle	
	180	220
Bolus Ratio With "Insert" – 2.4 cm air gap	2.05	1.81
Bolus Ratio With "Insert" -1 cm air gap	2.08	1.88

From the Table 4-2, the bolus ratios are shown for the simple insert model shown in Figure 4-5B. The difference between the bolus ratios obtained for the two different air gaps is small. A decrease of the ratio is seen with gantry angle. Similar to results shown in Figure 4-12, these bolus ratios are slightly different from phantom measurements results in Figure 2-9. This is discussed more in limitations section of Chapter 5 The bolus ratio will most likely be less than 1.8 in a clinical setup since gantry angles ranged from 230-260.

4.3.3 Patient Case Simulation

Figure 4-17 shows the dose distriubtions for a patient case that was calculated in Eclipse and in EGSnrc. Both the TPS plan and MC simulation has the insert incoporated into the dose computation. The red circle in Figure 4-17B outlines the difference in dose distributions reported by the two. Figure 4-18 shows the difference between the MC dose distribution and the Eclipse dose distribution. The displayed color dose isodose line range was minimized to show the potential hot spot for this patient. Where these hot spots could occur depend on the distance between the patient skin and the insert since there is a foam cushion in between. From the results in Table 4-2, there was little difference between a simulated foam cushion thickness of 2.4 and 1 cm. Most probable hot spot areas will be areas around the cutout of the insert where they could be incorporated into treatment fields.

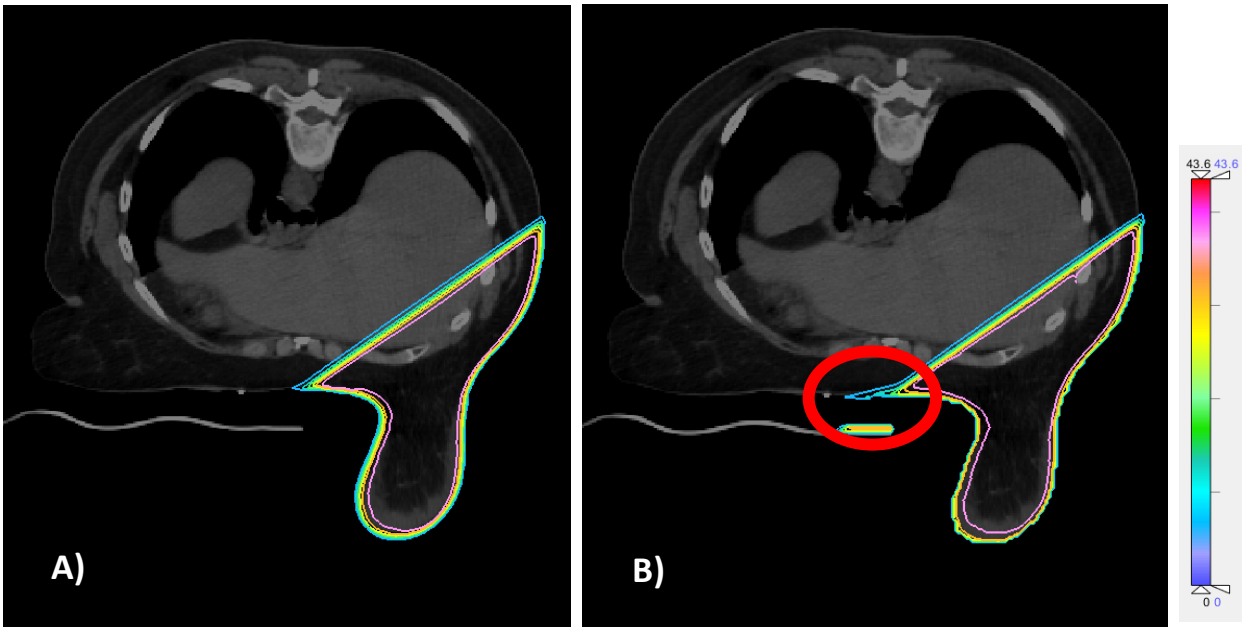

Figure 4-17: Isodose distributions of a patient case in CERR, eclipse calculated (A) and MC calculated (B).

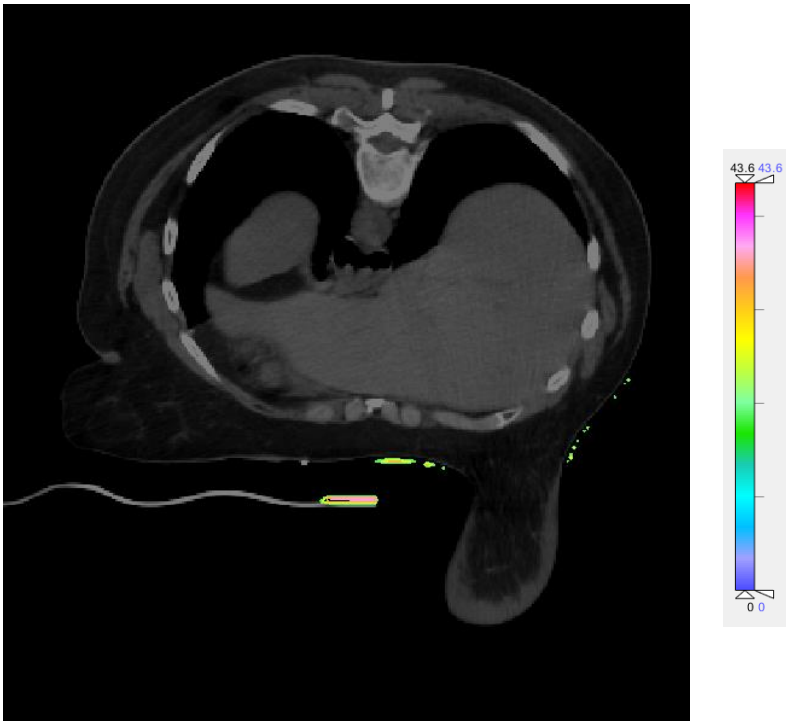

Figure 4-18: Subtraction between MC calculated and Eclipse calculated doses displayed in CERR.

4.4 Summary

Results have demonstrated that MC is able to provide better dose information than what is seen in the TPS. However for the accurate results, materials with densities most closely matching actual physical materials should be determined so that external devices can be properly modelled in patient simulations. The effect that the air gap has with shallow depth doses that was seen in Chapter 2 Section 2.3.3 was also mirrored in MC simulations. The scatter analysis used for phantom simulations show that the scatter component of a dose at the surface with the board base can contribute an additional dose up to around 45 cGy with a 0 cm air gap to the reference surface dose of 43 cGy. An example patient case with the prone breast board insert incorporated showed a potential hot spot located in the midline chest area over the treatment course. Using the same MC simulation work flow, other external structures such as the board base along with the couch structures can all be incorporated for clinical treatment evaluation, especially when skin dose is of potential concern due to close proximity with the board base or close contact with the insert.

Chapter 5: Final Summary and Future Studies

5.1 Overall Summary

As stated in Chapter 1, the motivation of this dissertation was the need to quantify the dosimetric effects of the immobilization board and couch structures in prone breast radiation. This was important to do so since neither of these external structures were taken into consideration into treatment plans traditionally. Results from Chapter 2 showed that both the components of the breast board and couch structures attenuate the beam, especially the couch top which could cause over 10% attenuation. Close proximity to the board base and contact with the insert also resulted in an increase of the surface dose. Attenuation and increased surface doses could have clinical implications. Chapter 3 moved on to determine the clinical significance of the phantom study results in Chapter 2. A sample of patients chosen demonstrated significant compromise in target and WB coverage in multiple scenarios involving various board-couch combinations. This stresses the importance of having both structures modelled during the treatment planning process. The feasibility and process of creating a custom support model of the prone breast board in a commercial TPS was shown later in that chapter. This model allows easy inclusion of the board to any treatment plan without manually contouring the structure for each patient. Correction of the attenuation effect which lead to insufficient coverage of the target and WB was also demonstrated via generation of a new clinically acceptable plan. Chapter 4 was a further investigation of the scatter and bolus effects of the breast board by utilizing MC calculations to provide more information about doses in the buildup region which was not possible in the TPS. The trends that were seen in the initial phantom study in Chapter 2 were also seen in MC calculations as well a dose enhancement to the surface due to the insert.

5.2 Limitations and Future Studies

Parts of this study (i.e. Chapter 2) involve looking at the buildup region or surface (i.e. scatter and bolus effect). There are many limitations and factors which influence results of measurements performed in the buildup region. Since charged particle equilibrium doesn't exist in the buildup region, dose information cannot easily be determined from ion chamber measurements. The detector chosen to perform the measurement is also important. Factors to take into account should be angular dependence, effective depth of measurement, energy dependence and etc. (15) The "gold standard" for surface dose measurements is the use of an extrapolation chamber, but this may not always be available. An alternative is the parallel plate chamber but this chamber is subject to a polarity effect as well as perturbations with obliquity (15). In additional to parallel plate measurements, results that were obtained can be supplemented by other measurements such as film. Film provides dose information along a whole plane rather than a point and has higher spatial resolution (15). This is useful for characterizing the dose distribution along the area where a patient is in contact with the breast board. Other studies referenced in TG 176 have also used other detectors such as diodes, thermoluminescent dosimeters or optically stimulated luminescent detectors being used for surface dose measurements (15). In vivo measurements or clinical treatment notes would also provide information about potential doses or situations where skin reactions could occur.

Most measurements performed were for the energy 6 MV, which is primarily mostly being used clinically with the exception of certain cases using a combination of 6 MV and 23 MV or 10 MV. The phantom studies could be expanded to include these. Currently, only the 6 MV energy was modelled in the Trilogy linear accelerator model in EGSnrc. Again, expanding the current 6 MV to 10 MV and 23 MV should also be considered to reflect the complete spectrum of clinical plans. Limitations of the custom

model are as mentioned in Chapter 3 including resolution of structures and this will affect the shape of the structure if resizing of the CT image has to be done or if structures have to be moved excessively.

Future works for Chapter 4 which entails running additional patient simulations with varying portions of the board and insert in the treatment field to provide information about any correlation between increased skin doses and potential skin reactions for treatment management. Further verification of the attenuation effect for couch models in the TPS could be done with MC simulations because of the discrepancies seen between measured and TPS calculated transmission factors. Another aspect that could be looked at is the scatter effect in combination with couch tops which also act a scatterer.

Other future works could be the development a solution that would mitigate any potential skin reactions that occur due to the board base or insert. The methodology outlined in this dissertation also can serve as a general guideline that can be applied to other immobilizations devices and their clinical implementation. On a further note, other materials could be studied and one could develop their own in-house immobilization device.

References

1. Bailar JC, Hoogstraten B. *Breast Cancer*. Berlin: Springer; 1989.

2. "Breast Cancer." American Cancer Society. https://www.cancer.org/cancer/breast-cancer.html.

3. Cancer of the Breast (Female) - Cancer Stat Facts. SEER. https://seer.cancer.gov/statfacts/html/breast.html

4. Veronesi, Umberto et al. Twenty-Year Follow-up of a Randomized Study Comparing Breast-Conserving Surgery with Radical Mastectomy for Early Breast Cancer. *New England Journal of Medicine* 2002; 347(16): 1227-232.

5. Jacobson, Joan A et al. Ten-Year Results of a Comparison of Conservation with Mastectomy in the Treatment of Stage I and II Breast Cancer. *New England Journal of Medicine*.1995; 332(14): 907-11.

6. Martin LJ. Lumpectomy (Partial Mastectomy): Purpose, Procedure, What to Expect. WebMD. https://www.webmd.com/breast-cancer/lumpectomy-partial-mastectomy.

7. Sarrazin, D. et al. Ten-year Results of a Randomized Trial Comparing a Conservative Treatment to Mastectomy in Early Breast Cancer. *Radiotherapy and Oncology.*1989; 14(3): 177-84.

8. Mamounas, Eleftherios P. NSABP Breast Cancer Clinical Trials: Recent Results and Future Directions. *Clinical Medicine and Research*.2003; 1(4): 309–326.

9. Fisher, Bernard et al. Twenty-Year Follow-up of a Randomized Trial Comparing Total Mastectomy, Lumpectomy, and Lumpectomy plus Irradiation for the Treatment of Invasive Breast Cancer. *New England Journal of Medicine*.2002; 347(16): 1233-241.

10. Merchant, Thomas E., and Beryl Mccormick. Prone Position Breast Irradiation. *International Journal of Radiation Oncology*Biology*Physics.* 1994;30(1):197-203.

11. Huppert N, Jozsef G, Dewyngaert K, Formenti SC. The role of a prone setup in breast radiation therapy. *Front Oncol*. 2011;1(31):1-8

12. Stegman, Lauren D. et al. Long-term Clinical Outcomes of Whole-Breast Irradiation Delivered in the Prone Position. *International Journal of Radiation Oncology*Biology*Physics.*2007;68(1): 73-81.

13. Whelan, Timothy J et al. Long-Term Results of Hypofractionated Radiation Therapy for Breast Cancer. *New England Journal of Medicine*.2016;362(6): 513-20.

14. Haviland, Joanne S et al. The UK Standardisation of Breast Radiotherapy (START) Trials of Radiotherapy Hypofractionation for Treatment of Early Breast Cancer: 10-year Follow-up Results of Two Randomised Controlled Trials. *The Lancet Oncology.*2013;14(11): 1086-094.

15. Olch, Arthur J. et al. Dosimetric Effects Caused by Couch Tops and Immobilization Devices: Report of AAPM Task Group 176. *Medical Physics.*2014;41(6):1-30.

16. Wagner D, Vorwerk H. Treatment Couch Modeling in the Treatment Planning System Eclipse. *Journal of Cancer Science & Therapy*. 2011;3(1):7-12.

17. Becker S, Patel R, Mackie T. Increased Skin Dose With the Use of a Custom Mattress for Prone Breast Radiotherapy. *Medical Dosimetry*. 2007;32(3):196-199.

18. Kinhikar RA, Sharma PK, Patkar S, Tambe CM, Deshpande DD. Electronic tissue compensation achieved with both dynamic and static multileaf collimator in eclipse treatment planning system for Clinac 6 EX and 2100 CD Varian linear accelerators: Feasibility and dosimetric study. *Journal of Medical Physics.* 2007;32(2):56-59.

19. Friend, M. An Overview of Electronic Tissue Compensation (ECOMP) for Breast Radiotherapy. Poster presented at: 2014 Combined Scientific Meeting (CSM) on Imaging and Radiation in Personalised Medicine; 2014; Australia.

20. Yoo S, Horton J, Yin F, Blitzblau R. Dosimetric Effect of the Prone Breast Board and the Couch Top for Whole-Breast Treatment in Prone Position [ASTRO abstract 2113]. *International Journal of Radiation Oncology*Biology*Physics*. 2015; 93(3)(Suppl):E46-47.

21. De Puysseleyr A, De Neve W, De Wagter C. A patient immobilization device for prone breast radiotherapy: Dosimetric effects and inclusion in the treatment planning system. *Physica Medica.* 2016: 32(6): 758-766.

22. Emmens DJ, James HV. Irregular Surface Compensation for Radiotherapy of the Breast: Correlating Depth of the Compensation Surface with Breast Size and Resultant Dose Distribution. *The British Journal of Radiology*. 2010;83(986): 159–165.

23. Seco J, Verhaegen F. *Monte Carlo Techniques in Radiation Therapy*. Boca Raton: CRC Press; 2016.

24. Bjarngard, B., and Frank H. Attix. "The dosimetry of ionizing radiation." (1990): 427-539.

25. "The Monte Carlo Simulation of Radiation Transport" https://www.aapm.org/meetings/06SS/documents/kawrakow_MonteCarlo_color.pdf

26. "DOSXYZnrc Users Manual". https://nrc-cnrc.github.io/EGSnrc/doc/pirs794-dosxyznrc.pdf

27. Panettieri, V., Barsoum, P., Westermark, M., Brualla, L., & Lax, I.. AAA and PBC calculation accuracy in the surface build-up region in tangential beam treatments. Phantom and breast case study with the Monte Carlo code PENELOPE. *Radiotherapy and oncology*.2009; *93*(1), 94-101.

28. Guebert A, Conroy L, Weppler S, et al. Clinical implementation of AXB from AAA for breast: Plan quality and subvolume analysis. *J Appl Clin Med Phys*. 2018;19(3):243-250.

29. Bray FN, Simmons BJ, Wolfson AH, Nouri K. Acute and Chronic Cutaneous Reactions to Ionizing Radiation Therapy. *Dermatol Ther (Heidelb)*. 2016;6(2):185-206.

30. Amato, Ernesto & Lizio, Domenico & Baldari, S. Applications of the monte carlo method in medical physics. *Medical Physics*. 2013; 105-113.

31. "McGill Monte Carlo Treatment Planning Users Manual". https://andrewwalexander.github.io/MMCTP/download/MMCTPUsersManual.pdf

32. Bhagroo, S, et al. Secondary monitor unit calculations for VMAT using parallelized Monte Carlo simulations. *Journal of applied clinical medical physics.*2019; 20(6): 60-69.

33. Gray, A., Oliver, L.D. and Johnston, P.N. The accuracy of the pencil beam convolution and anisotropic analytical algorithms in predicting the dose effects due to attenuation from immobilization devices and large air gaps. *Med. Phys*. 2009; 36(7): 3181-3191.
34. Formenti SC, DeWyngaert JK, Jozsef G, Goldberg JD. Prone vs Supine Positioning for Breast Cancer Radiotherapy. *JAMA*. 2012;308(9):861–863.
35. "Interaction of Gamma Radiation with Matter". https://www.nuclear-power.net/nuclear-power/reactor-physics/interaction-radiation-matter/interaction%20-gamma-radiation-matter/
36. "PENELOPE-2014: A Code System for Monte Carlo Simulation of Electron and Photon Transport" https://www.oecd-nea.org/science/docs/2015/nsc-doc2015-3.pdf
37. Qfix.ClearVue Prone Breast Device (Brochure). https://qfix.com/sites/default/files/M085_Sell%20Sheet,%20Access%20ClearVue_0.pdf